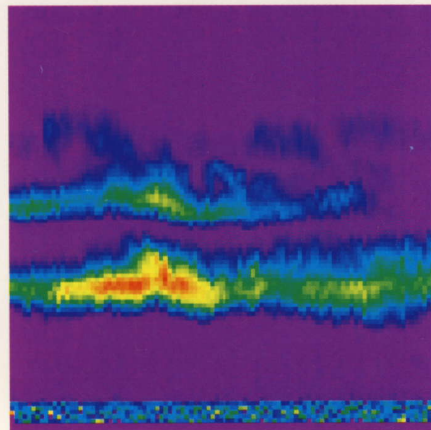
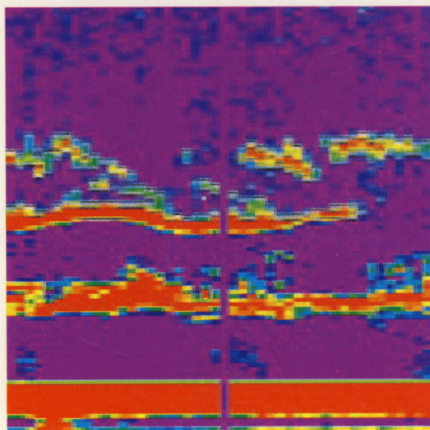
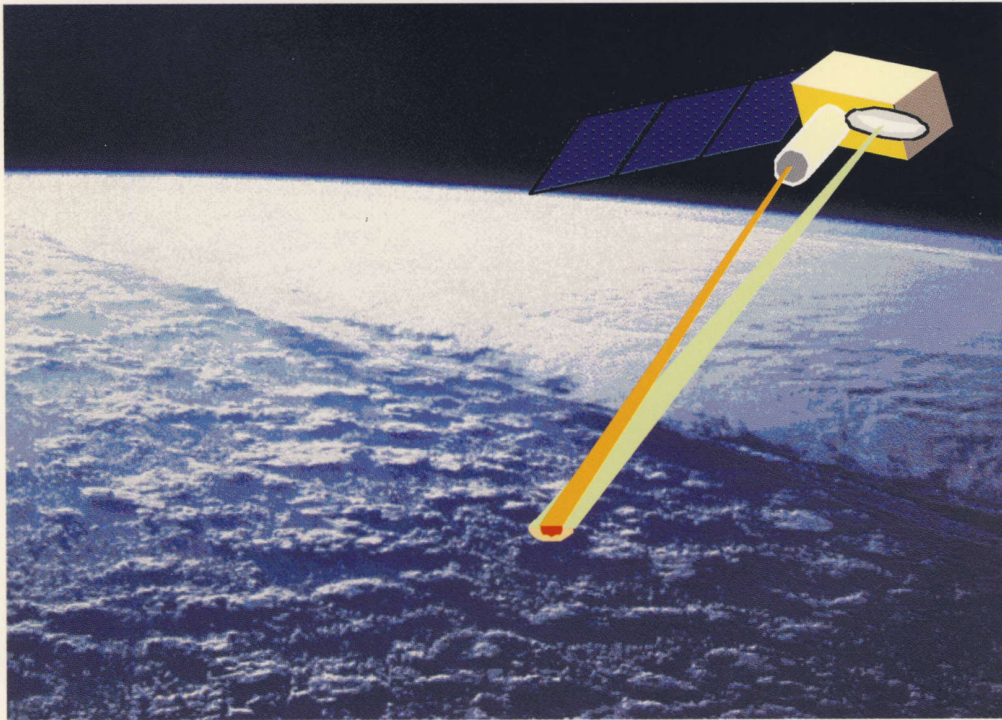




99P0A1-D011

# *3D-CLARE*

Three Dimensional Cloud - Aerosol - Radiation Budget Experiment  
(proposal of ATMOS-B1 Mission)



ATMOS-B1 Team,  
Cloud, Aerosol and Radiation Budget Science Team  
Committee for Earth Observation Systems  
Earth Science and Technology Forum

Earth Science & Technology Organization

**3D-CLARE**  
**Mission objectives and scientific requirements of**  
**ATMOS-B1 program**

**Contents**

1. Introduction .....	1
2. Scientific Issues .....	4
2.1. Radiation Budget .....	4
2.1.1. Clouds .....	4
2.1.2. Aerosols and the interaction with clouds .....	6
2.2. Water cycle and the Energy transfer .....	10
2.2.1. Water cycle .....	10
2.2.2. Energy Transfer .....	11
2.3. Climatology .....	13
2.3.1. Clouds .....	13
2.3.2. Aerosols .....	20
3. Scientific requirements for ATMOS-B1 mission .....	22
3.1. Cloud Processes in the GCM .....	22
3.2. Cloud-water cycle .....	23
3.3. Radiation Budget and cloud .....	24
3.4. Polar cloud and radiation .....	25
3.5. 3-Dimensional distribution of cloud and aerosol .....	26
3.6. Cloud-aerosol interaction .....	27
3.7. Summary .....	28
4. Mission Scenario .....	31
4.1. Sensors .....	31
4.1.1. Cloud profiling Radar(CPR) .....	31
4.1.2. LIDAR .....	38
4.1.3. Imager for cloud mapping .....	45
4.1.4. FTIR .....	46
4.2. Supporting data (ancillary data) .....	50
4.3. Orbit .....	51
References .....	54

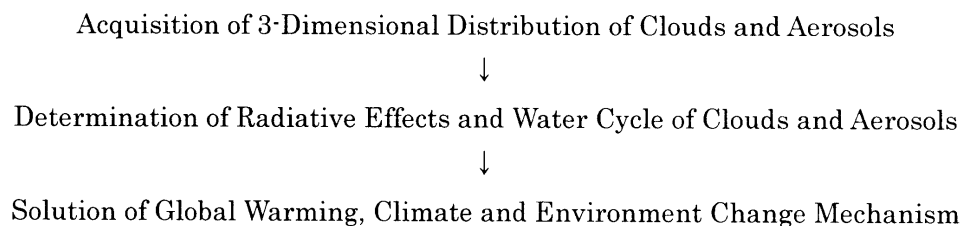
## 1. Introduction

In order to solve the global environment, climate change, and especially problems of the greenhouse warming, it is necessary to understand the behavior of clouds and their radiative effect. To the earth-atmosphere system, clouds generally increase planetary albedo, namely, reflection of incoming solar radiation at the top of the atmosphere, and bring cooling; but can also cause a greenhouse effect by trapping terrestrial radiation from the ground and result in heating. Warming can be either accelerated or suppressed, depending on the optical properties of clouds, whether global cloud amount either increases or decreases, or the three dimensional structure of cloud changes. It is most important to understand these trends of cloud behavior e.g., the three-dimensional distribution of clouds.

In addition to clouds, aerosols, suspended particles in the atmosphere, are also an important factor that can affect climate through directly increasing the reflection of solar radiation, or through indirect effect by acting as a nuclei for condensation of clouds. For this reason it is necessary to understand their behavior too.

To achieve the objectives described above, it is necessary to observe spatial configuration of clouds and aerosols by a satellite (ATMOS-B1) carrying a cloud profiling radar (CPR), a back scattering lidar, a cloud imager and a FTIR. We believe that this proposal will conform and contribute to the international co-operative research, such as WCRP/GEWEX, CLIC, ACSYS and IGBP.

The basic flow of the study in this proposal is as follows;



(Scientific significance)

Through acquiring the 3 dimensional distribution of clouds, cloud behaviors can be understood depending on the climate change such as global warming. The role of clouds on radiation budget and water cycle can be investigated, and then it will be clarified whether clouds will either accelerate or suppress greenhouse warming due to CO<sub>2</sub> increase.

Clouds are the largest factor in the climate system to decide the radiation budget of the earth-atmosphere system. However, since the distribution and variation of clouds were not certain, we could not understand the role of clouds in the climate change, which must be one of the important processes of the greenhouse warming. By acquiring the three dimensional distribution of clouds, one of the mechanism of climate change, namely the process of global warming, would be realized, together with the radiative effect of clouds. Also, realizing another factor of clouds to integrate the atmospheric water vapor and to originate a precipitation, we could understand the effect of clouds to the global water cycle. To acquire a reliable 3 dimensional cloud climatology will contribute to validate the cloud formation performance of GCM climate model, to improve climate model and then to the future prediction of the global climate.

Aerosols also have a certain distribution, vertical and horizontal, in the troposphere and stratosphere, in the global scale. Radiative properties of aerosols are variable, partly depending on the origin, natural, that is marine, soil and volcanic, or anthropogenic, and depending on the physical characteristics and chemical composition. Most of aerosols act to cool the earth-atmosphere system by increasing a solar reflection; however, even directly, some will warm the system through their absorption of radiation. It is confirmed by the climate model that a cooling effect of aerosols is unnegligible compared with the warming effect of greenhouse gases. An interaction of aerosols with clouds is another essential subject to be studied.

(Social effectiveness and urgency)

Social impacts caused by global warming are serious and immeasurable. Examples of impacts are countless, as seen in changes in agricultural environment, such as humidification or desertification through changes of precipitation pattern, and the sea level rise due to expanding of water, melting of glaciers and ice sheets in the polar regions. In order to predict the crisis, the future global environment, it is necessary first to understand these phenomena and to know precisely the mechanism of climate system. Since behaviors of clouds and aerosols were only known partly and insufficiently, thousands of different results have been obtained from the prediction using climate models. However, model performances can be improved and more realistic prediction of the future climate will become possible if behaviors of clouds and aerosols are well understood.

The Intergovernmental Panel on Climate Change (IPCC) was established by the United Nations in 1988. Various activities, including evaluation of methods to

predict climate change and of impacts of climate change have been discussed by the panel (IPCC, 1996), and the Framework Convention on Climate Change (FCCC) was adopted in 1992. Various measures have already been ready for immediate execution to prevent global warming. One of the examples is the Kyoto agreement, signed in 1995, as the international policy of restriction of anthropogenic emission of CO<sub>2</sub> to prevent the increase of atmospheric CO<sub>2</sub> concentration. Under such a background, advanced results of scientific studies on global warming are urgently required. There is a strong need to solve the mysterious behavior of clouds and aerosols to understand the mechanism of global warming.

## 2. Scientific issues

### 2.1. Radiation Budget

#### 2.1.1. Clouds

Clouds cover about 50% of the earth, thus having a strong influence on the earth radiation budget. Of the incoming solar energy, about 17% are reflected by clouds, and 4% are absorbed by clouds in mean annual, global average (Liou, 1992). The loss of terrestrial radiation to space is decreased by absorption in clouds. Thus clouds have two different aspects: one shades sunlight and cools off the earth, and the other warms the earth by absorbing infrared radiation from the terrestrial surface. What involved it is, that clouds can cool off or heat up the earth and change the radiation budget on the earth, depending on the cloud's characteristics. This is the reason why one of the greatest uncertainties in the study of climate change is the effects of clouds on the earth radiation budget.

Shortwave cloud radiative forcing principally arises from low and optically thick clouds, while longwave cloud radiative forcing is largest for upper and optically thin clouds. The role of clouds can easily switch from heating to cooling, depending on the altitude of clouds (Fig.1, Arking,1990). In addition, it has become clear from recent studies of radiative transfer simulations, that vertical distribution of detailed physical quantities, such as cloud particle size distribution, cloud droplet phase, and cloud overlap statistics, are very important for the radiation budget of cloud as well. For example, clouds composed of smaller droplets indicate higher albedo in the solar wavelength than those of larger droplets with the same liquid water contents. The earth radiation budget can change drastically depending on these conditions. It is said that the effect of such behavior is greater than the impact of increased carbon dioxide (Morcrette and Fouquart, 1986).

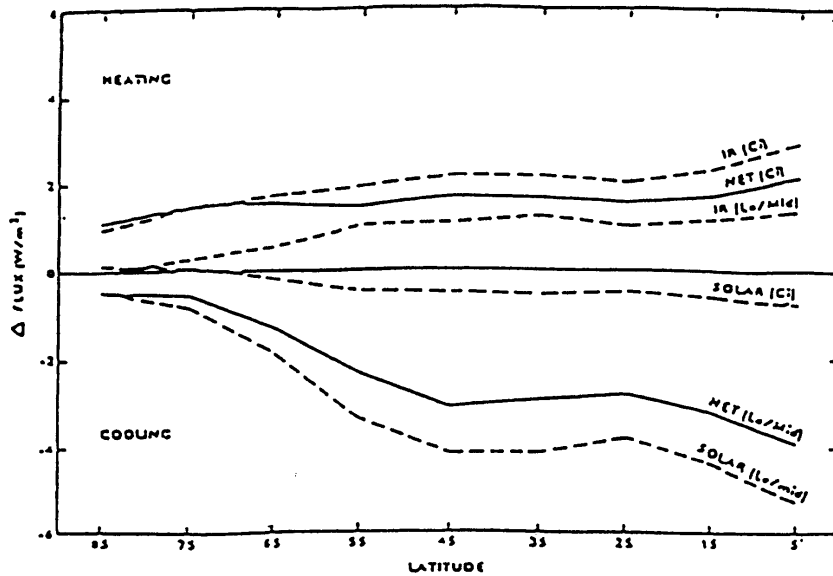


Fig.1. Change in the globally averaged annual mean flux into the earth-atmosphere system resulting from a 10%(relative) increase in cloud amount for cirrus(Ci) and for all other clouds(Lo/Mid),show for shortwave(SOLAR), longwave(IR), and net(NET) radiation components(Arking, 1990).

Upper clouds such as cirrus clouds have large longwave cloud forcing and hence warm the earth-atmosphere on annual average as mentioned above. However, the warming effect will be canceled by larger shortwave cloud forcing if the optical thickness of upper clouds is large. Since high clouds appear in cold temperatures and high altitudes, both observations of their microphysical properties by the passive instruments from the ground and from aircraft are extremely difficult. As upper level clouds consist of ice crystal particles, their optical characteristics are complicated and are not well known.

Cloud's structure varies widely in time and space. Horizontally inhomogeneous clouds often appear in nature and can greatly affect the radiation budget of clouds. For example, inhomogeneous clouds reflect less radiation than homogeneous clouds in same liquid water. These effects are not currently included in parameterization schemes for cloud-radiative interactions used in global circulation models. Parameterizations of these effects for GCMs are already constructed (e.g. Kobayashi, 1988), but it is necessary that parameterization of inhomogeneous cloud are validated with observation data.

If this proposed mission, mounted with CPR, lidar and related sensors can be achieved, it will greatly contribute to determine the three-dimensional structure of clouds described above. The CPR is able to measure the vertical structure of clouds, including cloud tops, bottom of clouds and vertical profiles of the optical characteristics (Clothiaux, 1955). Overlapped clouds can also be measured, unless the middle layer of the cloud is too thick. From observation at two or more wavelength, data on cloud particle distribution can be obtained to some extent. In addition, it will become possible to compute the radiation budget on the earth's surface, which is very important as basic data on low altitude clouds that could not be observed by previous satellite (Frouin et al., 1988). The lidar is able to observe the fine structures of clouds in a vertical direction of thin cloud and horizontal irregularities of the cloud. Based on the results derived by combination of these two active instruments, a radiation amounts can be computed. It can be expected that these data, together with the radiation amounts observed by the GLI or the CERES, will contribute greatly to the prediction of global warming in the earth-atmosphere system.

#### **2.1.2. Aerosols and the interaction with clouds**

One of the most indeterminate factors in global warming prediction studies is the aerosol effect (IPCC 95, TAR). The effect includes the direct effect caused by modulating the radiation field directly and the indirect effect that modifies the cloud field through interaction between aerosols and clouds (Charlson et al., 1992). Despite the impressive simulation of observed temperature record by Hadley Center that shows a possibility of significant cooling by anthropogenic aerosols after the Industrial Revolution (Fig.2, Mitchell et al., 1995), estimated radiative forcing of the aerosol effect is largely varied depending on the model we use. The direct effect can be evaluated to a certain degree by knowing the increase in optical thickness of man-made aerosols. Current estimate of the radiative forcing of the direct effect is about  $-0.5 \text{ W/m}^2$  at the top of the atmosphere (Hansen et al, 1998; IPCC TAR). On the other hand, the indirect effect is scarcely understood because the mechanism of cloud modification is significantly complicated. Estimated values of the radiative forcing due to the indirect effect vary widely by researchers within range from  $0 \text{ W/m}^2$  to  $-2.0 \text{ W/m}^2$  (Hansen et al., 1998; IPCC TAR). This range is even larger than that of IPCC95. Most of the estimates have been performed with global climate models having aerosol processes. In spite of large effort, these models still have tuning parameters for large-scale parameterizations of cloud-aerosol interaction processes (Lohmann et al., 1997; Rotstayn, 1999) that are difficult to be assigned on global scale. It is an extremely

difficult task, for example, to assign the water affinity of aerosol polydispersion on global scale, because of complicated mixing of aerosols of different types (Fig.3).

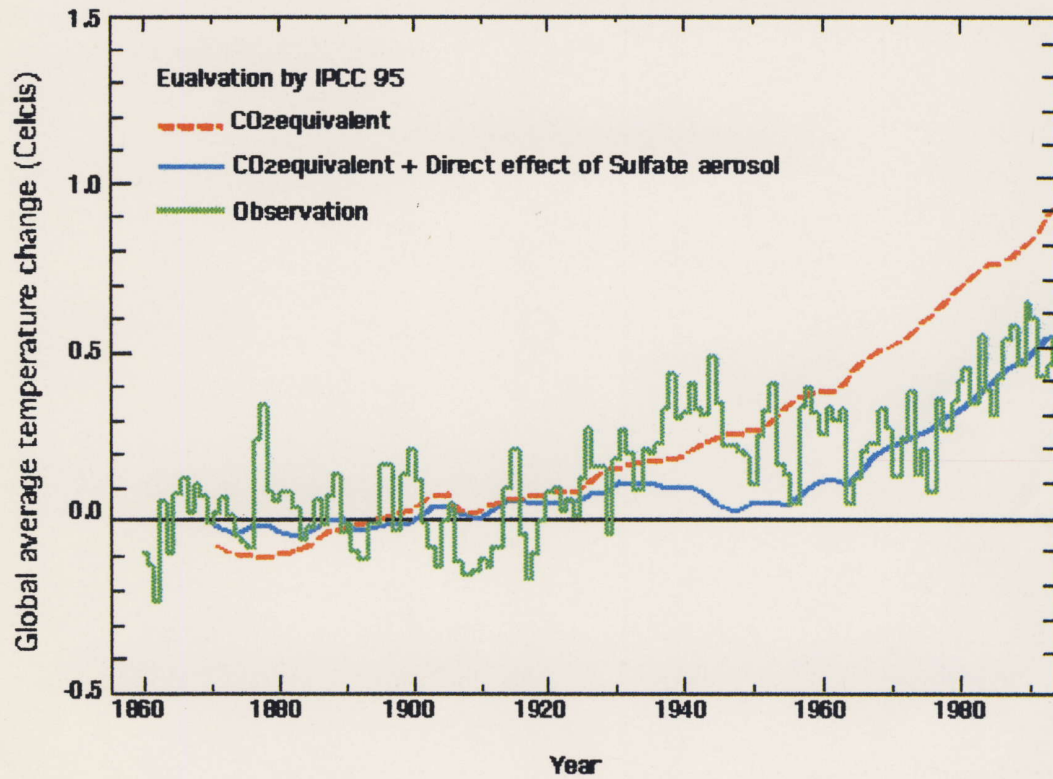


Fig.2. Time series of simulated and observed global surface mean temperatures (Mitchell et al., 1995).

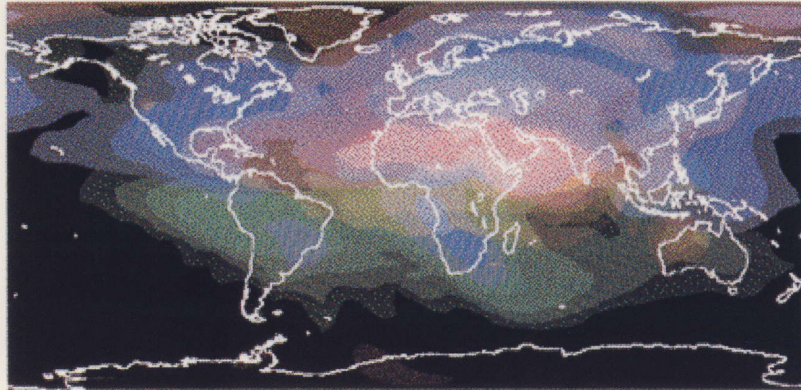


Fig.3. Simulation of global distribution of aerosol optical thickness with CCSR/NIES global climate model implemented aerosol generation/transport processes. Logarithm of optical thickness for each aerosol type of mineral dust (red), sulfate (blue), and carbonaceous (green) are shown. Case of July 1990.

In this situation, ground and satellite measurements have become important to provide data for improving the aerosol climate models. Especially, satellite remote sensing analysis provides geophysical parameters of clouds and aerosols relevant for cloud-aerosol interaction studies. Only one global distribution of the cloud effective particle radius was derived from AVHRR by Han et al. (1994) and widely used for model validation. However, such a passive remote sensing method largely depends on several assumptions in the algorithm. For example, Kawamoto et al. (2000) have obtained a similar distribution of the effective particle radius, but, at the same time, they found that a different cloud screening method can produce different results (Fig. 4). At the same time, it should be noted that these passive remote sensing methods derive, by its nature, only the effective particle radius near the cloud top. On the other hand, the magnitude of the aerosol indirect effect largely depends on the height within the cloud layer.

Cloud profiling by active sensors, such as CPR and lidar, will add an unique and useful information that is difficult to obtain by climate modeling and passive remote sensing. The vertical distribution of the effective particle radius will be obtained with combined analysis of radar and lidar signals, along with vertical distribution of the cloud liquid water content. From analysis of clear sky area, lidar will provide us with the vertical profile of aerosol concentration. Besides the indirect forcing of aerosols, the one large factor among the interaction between aerosols and cloud particles is the

wet deposition processes inside clouds. Since numerical studies by aerosol transport model has shown that aerosol concentrations is strongly influenced by the amount of clouds due to 'in-cloud scavenging' (Takemura et al., 2000), not only lidar but also CPR can be expected to contribute aerosol effects on the climate system in this regard.

cl

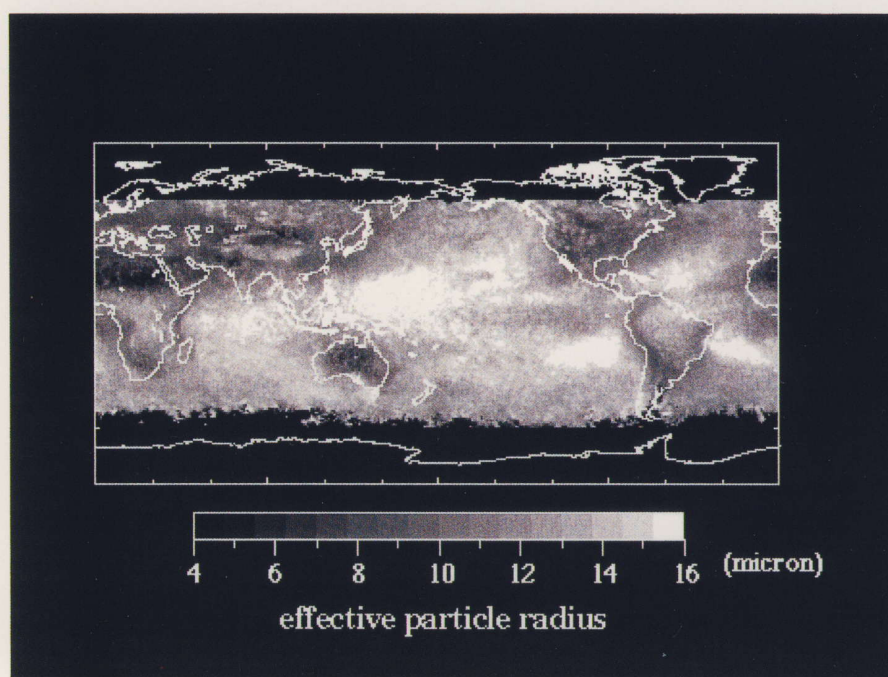


Fig.4. The global distribution of the cloud effective particle radius derived from AVHRR (Kawamoto et al., 2000). Annual mean of 1990 for low clouds with cloud top temperature larger than 273K.

## 2.2. Water cycle and the Energy transfer

### 2.2.1. Water cycle

Water vapor evaporated from ground and sea surfaces is carried away by the wind, condenses to form clouds at various altitudes, and evaporates or returns to the earth's surface as rain or snow. The speed of water cycle in the atmosphere depends on the ratio between the amount of cloud water (liquid and ice) and that of rain or snow, and on the rate at which cloud particles change into rain or snow in clouds. The former is called as a precipitation efficiency and the latter is called as a conversion rate. These two values differ largely among cloud systems. Especially in multi-layered cloud systems, properties of lower level clouds are largely affected by the upper level clouds (Houze and Hobbs, 1982). Recently, Chahine et al. (1997) and Trenberth (1997) defined an atmospheric moisture cycling rate as the ratio of the precipitation to precipitable water. Chahine et al (1997) suggested that this cycling rate may be increasing (Fig.5), Roads et al. (1998), however, suggested that the global warming could ultimately decrease the cycling rate, and noted that there are fairly large discrepancies among the observations, re-analysis and climate models.

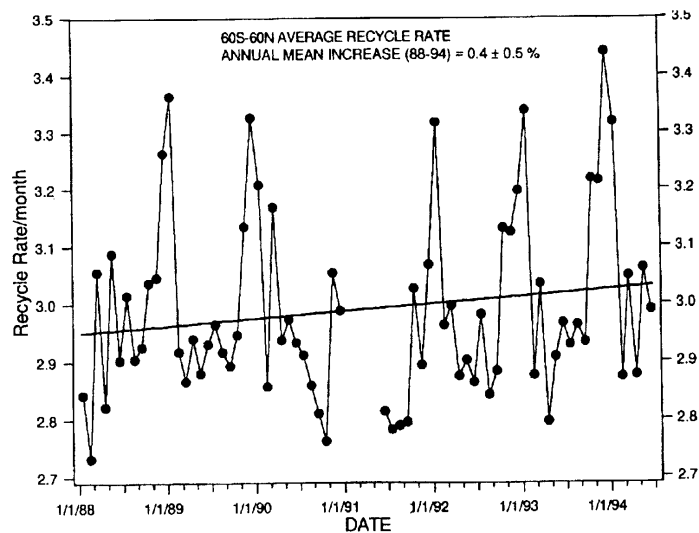


Fig. 5. Observed monthly variations and trend of the global recycling rate of the total precipitable water vapor for the period 1988-1994 between 60° S and 60° N. (Note missing precipitation data in 1991).

Currently, global circulation models (GCMs) use various kinds of schemes to parameterize precipitation efficiencies and conversion rates. The slower the speed of water cycle is, the farther water vapor is transported and the longer cloud droplets survive, resulting in increase in both cloud cover and cloud water content. Since the radiation budget of the earth greatly depends on the amounts of cloud cover and cloud water, determination of precipitation efficiencies and conversion rates of various kinds of cloud systems is an extremely important subject.

As a cloud structure changes temporally and spatially, a large number of observation points equipped with radar and lidar would be necessary to determine global climate values of precipitation efficiencies and conversion rates based on ground observation data. Conversely, if such equipment is mounted on a satellite, it is possible to cover wide areas including oceans. Vertically integrated liquid water content have already been measured by using SSM/I mounted on the US Defense Meteorological Satellite Program (DMSP) satellite, and the global distribution of vertically integrated water vapor amount are being measured. However, it is impossible to measure vertical structure of clouds and precipitation by using passive microwave radiometers. Only active sensors like radar and lidar can measure vertical distribution of ice/water. If these data are combined with data measured by ground-based radar, rain gauges, or a precipitation observation satellite such as TRMM, global climate values of precipitation efficiencies and conversion rates of various kinds of cloud systems would be obtained, and these values can be incorporated into numerical models.

### **2.2.2. Energy Transfer**

Although the lapse rate of the earth's atmosphere is well known by radiosonde measurements, it is impossible to simulate it. It is qualitatively understood that the observed lapse rate is different from dry adiabatic value or radiatively equilibrium value because diabatic heat exchange occurs in the atmosphere. Thus the diabatic heating or cooling rate in the atmosphere and its three-dimensional structure is quite important for the understanding of climate system. However, this has not been properly evaluated particularly for the cloudy atmosphere. Two major factors can be considered as causes for generating diabatic heating or cooling. One is heating or cooling by absorption and emission of solar and terrestrial radiation, and the other is output and input of latent heat due to change of phase of water (e.g. Peixoto and Oort, 1992). The effects of the latter become heating in most cases, because condensation is more prominent than evaporation in the atmosphere. There are some computed

results of heating and cooling rates, but the computations have actually been made using some assumptions including cloud parameters based on a limited number of observation data. As shown in Fig.6, if the altitude of the cloud bottom is different while the cloud top is the same, the distribution of heating or cooling rate by longwave radiation in the atmosphere can vary widely (Slingo and Slingo, 1988). Since information on lower level clouds and vertical distribution of clouds cannot be obtained from conventional satellite observations using visible, infrared, or microwave radiation from targets, it is extremely difficult to estimate precise distribution of radiative heating or cooling rates. The microphysics including the phase of particle within cloud is also important for both radiation budget and latent heat budget in the cloud.

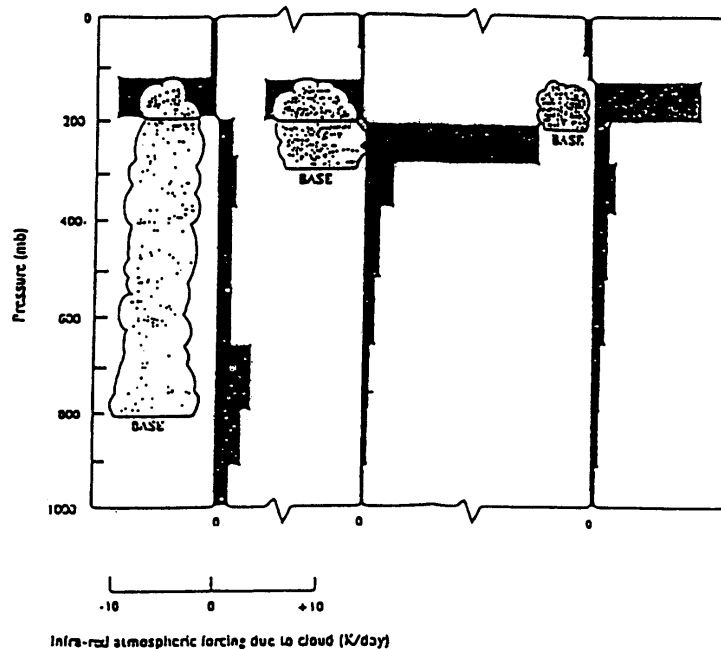


Fig.6. Variation of vertical heating rate for terrestrial radiation as a function of cloud base height (Slingo and Slingo,1988).

On the other hand, the atmospheric heating by latent heat, for example as seen in process of developing cumulonimbus clouds in tropical regions, can significantly affect the dynamics and plays an important role in the process of heat transport on the earth, that is, where energy of water vapor evaporated from the earth surface is released by condensation by cloud forming. As described above, it is difficult to observe directly the latent heat to be released due to condensation of water vapor, but

it will become possible to make more precise evaluation for where latent heat is released into the atmosphere, by combining with the simulation analysis of the three-dimensional cloud structure. Thus, if the vertical distribution of clouds is globally known, the preciseness of evaluations of three-dimensional distribution of radiation/latent heat in the atmosphere will be advanced significantly. For this purpose, observation system using active sensors such as a radar and a lidar is indispensable. Although these active sensors are extremely powerful in defining vertical cloud distribution, the horizontal coverage of these two active sensors are rather poor and also the absolute values of cloud parameters, such as optical thickness, water content etc, are slightly decisive. Therefore, it is necessary to carry out observations using also conventional passive type visible, infrared, or microwave sensors to complement the disadvantages.

## 2.3. Climatology

### 2.3.1. Clouds

Cloud distribution - cloud climatology - is one of the key parameter of the global climate. Without a knowledge of long range global distribution of cloud amounts, cloud types, cloud base/top heights, cloud constituents and cloud optical properties, it is impossible to proceed the study on earth radiation budget, global water cycle and climate change (Weatherald and Manabe, 1980). Thus, cloud climatology has been discussed for a long time. However, there exist no reliable cloud climatology till the present. It is of urgent need to originate a reliable cloud climatology from satellite observations.

Study on cloud climatology using satellite data has been started in 1960's, from the early stage of meteorological satellites. Cloud climatology is well known till then was that of London (1957). Due to lack of surface observation stations, over the ocean, deserts in the central part of continents, and so on, this climatology was not a reliable one throughout the globe. Arking (1964) derived the first latitude distribution of clouds by TIROS III visible data, and van Loon (1972) derived the cloud climatology in the Southern Hemisphere from the surface based and satellite data. Many works have been done in these fifty years have been compared by Hughes (1984) as shown in Fig. 7. Though there are quantitative difference among those results, latitudinal distribution seems to be rather similar. Warren et al. (1985, 1988) had made an extensive compilation of ground surface observed cloud parameters, as for the unique standard for the satellite observations.

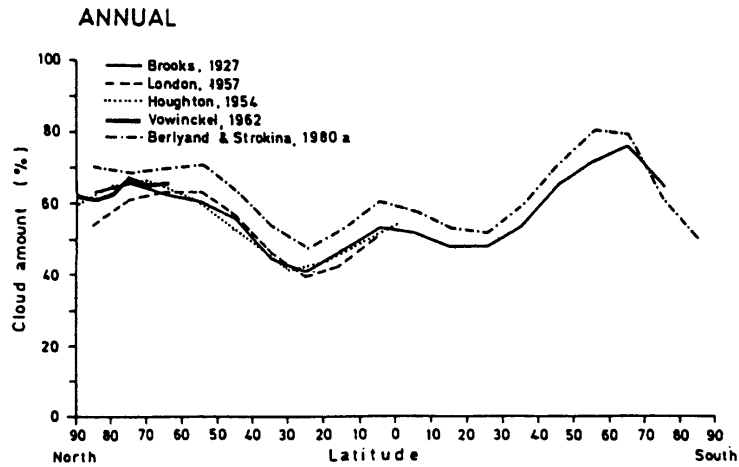


Fig.7. Meridional profiles of zonally averaged cloud amount for annual conditions from historical data (Hughes, 1984).

Although space-borne microwave radiometers such as SSM/I can measure precipitation, cloud water/ice and water vapor and became available in these ten years, they can provide only vertically integrated values over the ocean. Therefore, visible and infrared channels are useful to derive the global distribution of clouds. The basic algorithms are higher albedo and lower brightness temperature of clouds, compared to the ground surface/clear regions. Then the method using a threshold in the visible or infrared channels, method to compare the measured albedo or brightness temperature with the theoretical calculation, and the method to use a variability within a small area are mainly used. Nimbus-7 global cloud climatology is one of the major cloud climatology by satellite, obtained with THIR and TOMS data using bispectral threshold method during six years between 1979 and 1986 (Stowe et al., 1989).

Now the International Satellite Cloud Climatology Project (ISCCP) is the main project under the World Climate Research Programme (WCRP) to derive cloud climatology from satellite since 1983 (Schiffer and Rossow, 1983; Rossow and Schiffer, 1991). Behavior of clouds which controls the climate through earth radiation budget is one of the largest issue within the WCRP. Cloud data sets are to be compiled from the composite of geostationary satellites and polar orbiting satellites. Following the discussions made during years, reprocessing of the entire data sets are performed as ISCCP D data set (Doutriaux-Boucher and Seze, 1998; Rossow and Schiffer, 1999).

Though cloud derivation algorithms and cloud climatology from satellite data have gradually improved through the extensive study during these years, still there

exist large uncertainties in the cloud climatology in the polar regions (Yamanouchi and Kawaguchi, 1992; Curry et al., 1996) and also that of low clouds over the coastal ocean. For example, any of polar cloud climatology obtained from the surface observations or satellite observations does not coincide and is unreliable as shown in Fig.8 (Rossow et al., 1993). Even the surface observation is limited due to the sparseness of the stations and long polar night when the sky is difficult to be monitored by eyeball. In the polar regions, detection of clouds from satellite data is still very difficult. Since the ground surface is covered with snow or ice and the ground surface temperature is very low, the contrast in the visible albedo and the infrared brightness temperature is small between the ground surface and cloud top. In order to originate reliable cloud climatologies in the polar region, it is indispensable to develop a new method to detect cloud cover over the snow and ice surfaces, especially applicable for the long polar night. As for low level clouds, it is needed to be properly identified. Climatology for the low level clouds over the ocean at the west coast of the continent can be better understood.

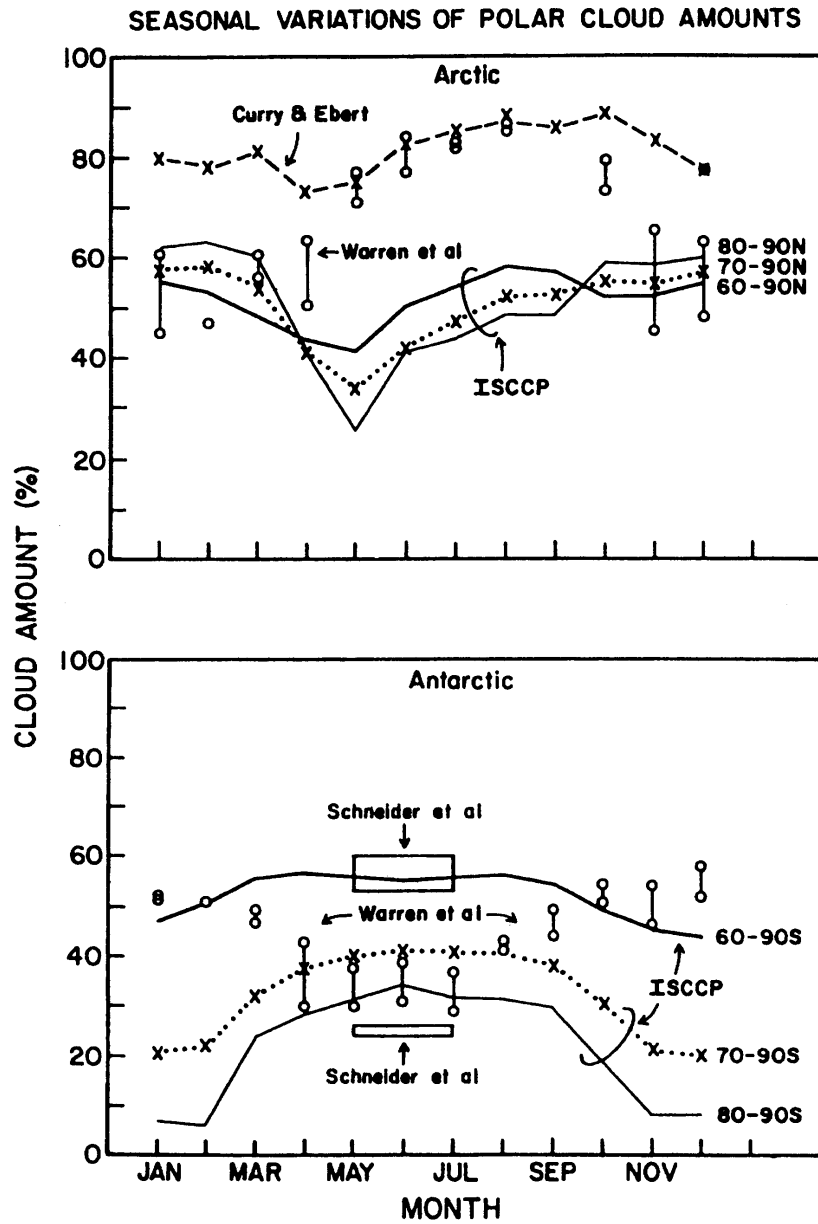


Fig. 8. Comparison of the seasonal variations of average cloud amount in the (a) Arctic and (b) Antarctic determined by ISCCP and other climatologies (Rossow et al., 1993).

The role of cloud is high in the high latitude and polar regions. From the latitude distribution of the cloud radiative forcing estimated from the satellite observations (Harrison et al., 1990) as seen in Fig. 9, the maximum distributes around  $\pm 60$  degrees. Although from this figure, the cloud radiative forcing seems to be small over Antarctica or the Arctic, these amounts are for the top of the atmosphere, and cloud radiative forcing at the surface is still large (Curry et al., 1996; Yamanouchi and Charlock, 1995). Also as foreseen by climate model studies, global warming due to the increase of carbon dioxide, is said to be enhanced in the polar region, as a result of several feedback mechanisms in the polar climate such as ice-albedo feedback. Clouds affect the growth and decay process of sea ice, and ice crystal precipitation dominated in the winter Arctic and Antarctic is also important for the radiation budget at the surface. The effect of clouds to the ice-albedo feedback related to the dependence of cloud distribution and sea ice or cloud radiative feedback is an issue to be solved. The cloud distribution over the ice sheet is a matter for discussion not only related to the radiation budget but also to the precipitation and accumulation. The strong impact of Antarctic clouds to the global climate has been demonstrated within whole Southern Hemisphere and even to the Northern Hemisphere through change in atmospheric circulation using GCM climate simulation (Lubin et al., 1998).

The Atmospheric Model Intercomparison Project (AMIP), initiated in 1989 under the WCRP, undertook the systematic validation, diagnosis, and intercomparison of the performance of atmospheric general circulation models (Gates et al., 1999). Although there are apparent model outliers in each simulated variable examined, validation of the AMIP models' ensemble mean shows that the average large-scale seasonal distributions of pressure, temperature, and circulation are reasonably close to what are believed to be the best observational estimates available. However, the total cloudiness is rather poorly simulated especially in the Southern Hemisphere and high latitude as seen in Fig. 10, for an example. If it is possible to measure clouds in the whole globe including low level ocean clouds and polar clouds precisely, it will greatly improve the understanding of climate mechanism, and then the performance of climate models.

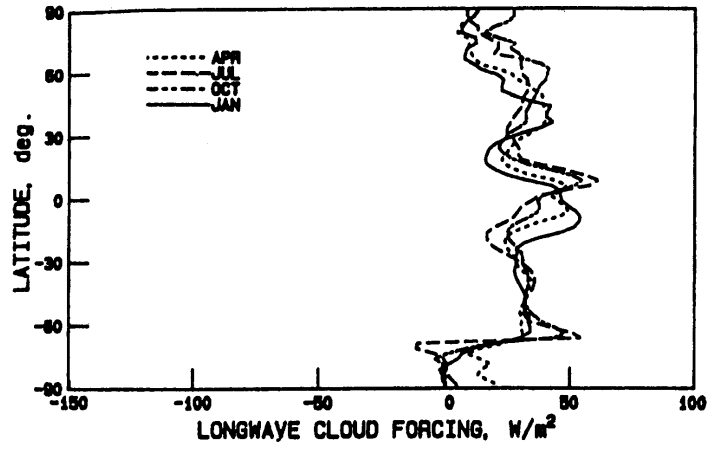


Fig. 1a

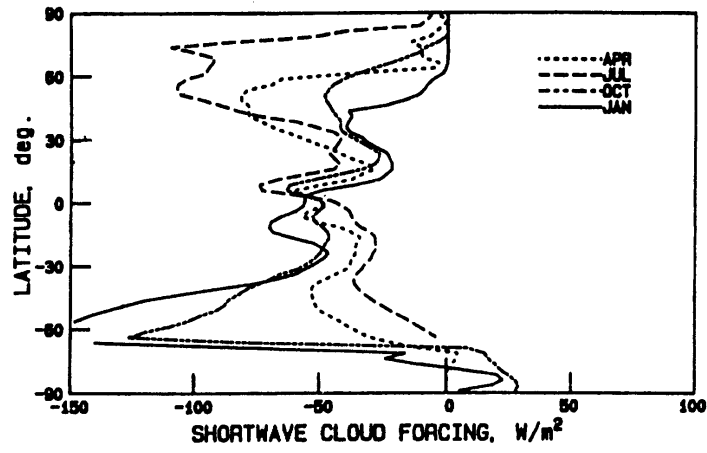


Fig. 1b

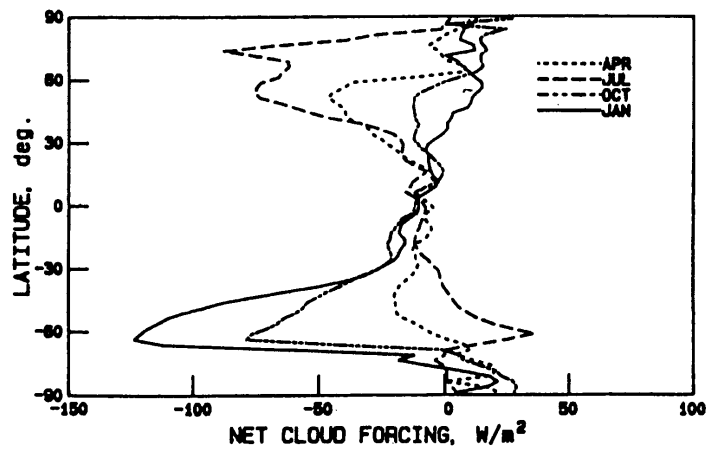


Fig. 1c

Fig. 9. Latitudinal variation of (a) longwave, (b) shortwave, and (c) net cloud radiative forcing from ERBE for April, July and October 1985 and January 1986 (Harrison et al., 1990).

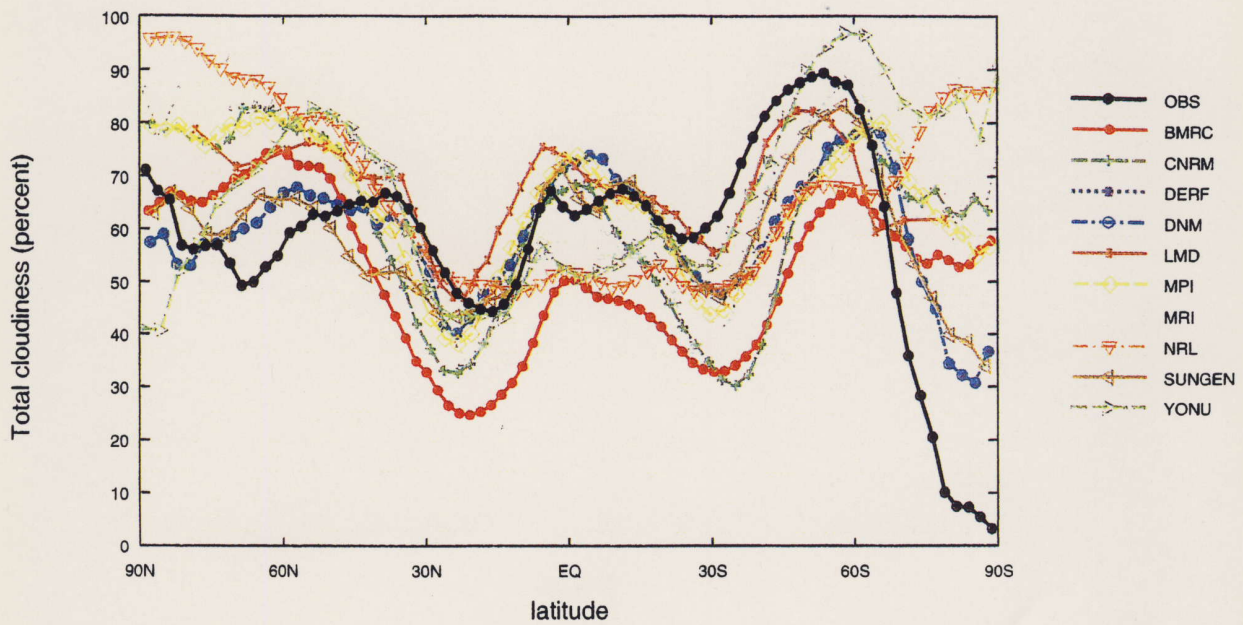


Fig.10. Zonally averaged total cloudiness simulated in December-January-February of 1979-88 by the subset of 10 models that revised AMIP with revisions, with the observed data from ISCCP for 1983-90 (Rossow et al., 1991) given by the solid line (Gates et al., 1999).

### 2.3.2. Aerosols

#### (1) Global Three-Dimensional Distribution of Aerosols

The direct effect of aerosols on solar radiation to the climate depends on the concentration and optical characteristics of aerosols. On the other hand, their indirect effect through cloud forming can vary based on the ambient water vapor pressure and the hygroscopic characteristics of aerosols. Average residence time of tropospheric aerosols is estimated to be from one week (for lower troposphere) to three weeks (intermediate and upper layers), but a continuous emission from various sources at the surface must give impact to the radiation environment. Highly concentrated aerosols in the lower atmosphere mainly take an important role in direct effect. It may be considered that aerosols in the intermediate and upper troposphere, where the residence time is relatively longer, play an important role in interaction with clouds although its direct optical effect is not so strong. The radiative forcing by aerosols may be estimated as a few watts (direct effect), and the total effect including cloud forming possibly may suppress a temperature increase due to the greenhouse effect. It is imperative that the aerosol effect should be properly evaluated in the climate study.

Increase of energy consumption required by an increase in human activities and advanced living environments can cause an increase in sulfur and nitrogen oxides in the atmosphere. These gases will turn into aerosols through gas-to-particle conversion process (GPC). Increased food production with an increase in human population can result in a lot of biomass burning which can generate a large amount of black carbon by incomplete combustion, as well as generation of sulfur oxide. Since the black carbon is optically absorptive, direct radiation effect of aerosols can possibly be reversed (greenhouse effect).

The global distribution of aerosols must be known in order to evaluate effects of aerosols on climate change. This information is, however, rarely available, for example, even the global distribution of optical thickness is still rough (Jaenicke, 1993). Particularly, information on vertical distribution is nearly nil. Vertical and horizontal transport of gaseous materials that are changed into aerosol through GPC process makes it easy for aerosol to reach upper atmosphere. Aerosols themselves are also transported widely through the global circulation system. In particular, since intermittent volcanic eruptions or dust storms can be a very large source of aerosol, such as examples of Mt. Pinatubo or Saharan dust, the transport process is important for climate system. It is believed that such events can greatly affect climate, depending on the place and size of event.

A lidar will give us very useful information of aerosol for global and three-dimensional structure. This will serve to develop global statistics of optical thickness, that has never been available in the past.

## (2) Stratospheric Aerosol

If spatial distribution of stratospheric aerosol can be obtained, it becomes possible to solve its conveyance and transformation processes, such as interaction with ozone and other minor components in the air, and impact on radiation budget.

Recently, it is recognized that the stratospheric aerosols are important in polar stratospheric clouds associated with ozone destruction in the polar region. Heterogeneous chemical reaction on the aerosol surfaces may contribute to the chlorine accumulation which modifies the ozone layer. After there is a huge volcano eruption and an abrupt increase in the stratospheric aerosols, even in the mid-latitude an ozone reduction might appear. Therefore it is important to monitor where and how the volcanic aerosols in the stratosphere are going on. Conversely, background aerosols in the stratosphere may consist of sulfates from the ocean and anthropogenic sources, and the global monitoring is required for the qualitative and quantitative estimation.

As a scattering ability in the stratospheric aerosols is smaller than that of clouds and tropospheric aerosols, it can be observed at night using a lidar with the degraded spatial resolution. Under normal conditions that are not affected by volcanic eruptions, fine scale observation is not required for stratospheric aerosols. Therefore, it can be expected that the global distribution of stratospheric aerosols, estimated by the lidar, will greatly facilitate the solution of sulfur circulation deemed as the origin of marine organisms.

When the amount of stratospheric aerosols increases significantly, heterogeneous chemical reactions on its surface become larger and can significantly reduce the stratospheric ozone. Such examples can be seen in polar stratospheric clouds or stratospheric clouds generated by volcanic eruptions. In such cases, optical thickness of stratospheric aerosol can greatly increase and a satellite-borne lidar will become possible with high resolution vertically and horizontally, not seen so far.

### 3. Scientific requirements for ATMOS-B1 mission

We have many science issues on aerosols and cloud related to the earth climate system described above. In order to understand the global climate system and its change, this satellite program will be focused on "the process study" of climate research. The earth radiation budget at the top of the atmosphere (TOA) and the surface is one of the important key parameters for climate research and its long range trend should be known. However, as well known, the ERBE scanners on NOAA 9 and 10 had observed the radiation budget at the TOA from 1984 to 1989 and the subsequent system named CERES has been launched by the TRMM. Moreover this will be continued for more than 10 years after TRMM by NASA. So, the climate itself, the long range trend of radiation budget, is not our main target.

Our objective of the satellite program is to clarify the mechanism of earth-atmosphere climate system. In the point of view, the effect of cloud and aerosols to the climate system through radiation budget and water cycle should be targeted at first.

#### 3.1. Cloud Processes in the GCM

Current GCMs still have a lot of uncertainties associated with cloud and aerosol radiation schemes. It is desired that the uncertainty of cloud and aerosol schemes is reduced through intensive validation with well-defined satellite observation.

The cloud and aerosol radiation causes a wide variety of large-scale phenomena in the atmosphere. The followings are processes in which cloud and aerosol radiations play significant roles. Concerning these processes, the model climate is very sensitive to cloud and aerosol radiation schemes.

(1) Asian summer monsoon is under strong influence of cloud and aerosol radiations. The solar insolation makes strong land-ocean heat contrast mainly because of the difference in the heat capacity and it triggers the monsoon circulation. Then, when the model is modified to enhance the cloud and aerosols over the land, it considerably delays seasonal march of the monsoon. The cloud aerosol schemes must be validated differently between over the land and over the ocean.

(2) Widely distributed oceanic low-level clouds strongly affect both the atmospheric and oceanic general circulations. They show strong positive feedback between the cloud radiation and cloud formation through the infrared cooling and the

enhancement of turbulent moisture transport, while they do negative feedback through the short wave heating. Both positive and negative feedback processes are very sensitive to cloud optical parameters, such as optical thickness, single scattering albedo and asymmetry factor. The validation of cloud diurnal variation is good to estimate the optical parameters.

(3) The cirrus clouds in the tropical upper troposphere show strong net radiative heating, although the cloud water is quite small. The cirrus cloud radiative heating considerably suppresses deep cumulus convections and enhances the upper tropospheric upward motion and mass exchange with the stratosphere. The cirrus clouds are so thin and broken that their cloud water, to be used for validation, is hardly observed. Note that the infrared heating is also sensitive to cloud height.

Table 1. Scientific requirements for GCM modeling

	resolution/accuracy	remarks
cloud amount	0.05 - 0.1	with cloud type, variance
cloud profile: height: density: LWP IWC	0.3km for near surface 0.01g/m <sup>3</sup> or (5g/m <sup>2</sup> )/500m TBD	
optical thickness of cloud	$\Delta\tau/\tau = 0.5 - 1$	
cloud phase	TBD	
optical thickness of aerosols	0.05	especially over land
resolution: horizontal	100 x 100 km <sup>2</sup>	
vertical	0.3km	dependent on altitude
Observation duration	2yrs + 1yr if available	

### 3.2. Cloud - water cycle

The conversion rate from cloud water/ice to rain/snow water changes largely depending on the horizontal scale and the types of cloud systems. It depends not only on microphysical properties of clouds but also on the multi-layer structure of cloud systems. Conversely, the period of duration of clouds and the amount of precipitation are closely related to the conversion rate.

Although many researchers have parameterized and estimated this value in their numerical models, only a limited number of observational studies have reported these values. Especially, there are no reports on its global distribution and its temporal change. Unfortunately, we cannot simultaneously measure these values by using any artificial satellites at the present moment. Therefore, the Atmos-B1

program will provide the global maps of rainfall/snowfall intensity as well as cloud water/ice amounts and their vertical profiles to calculate the conversion rate.

Table 2. Scientific requirements to calculate the conversion rate

parameters	resolution/accuracy	remarks
rainfall / snowfall intensity	$< 2 \text{ mm hr}^{-1}$	The conversion rate will be estimated by the aid of meso-scale cloud resolving models. Also these values are used to verify and improve these meso-scale models and regional-scale models.
cloud water /ice content	$< 0.2 \text{ g kg}^{-1}$	
cloud layering	necessary	
cloud type	stratiform / convective	
phase of particles	ice / water	
cloud top/ bottom temperature	$< 1 \text{ K}$	
Observation duration	2yrs + 1yr if available	
resolution	horizontal: vertical:	
	1km x 1km <0.5 km	

### 3.3. Radiation Budget and cloud

Current problems:

Vertical distribution of clouds greatly affects the radiation budget. Vertical distribution of cloud particles, liquid water contents and ice water contents determine the divergence of radiative fluxes and heating or cooling of the atmosphere, and also radiative fluxes at the TOA and the surface. The surface radiation budget is especially sensitive to the height of cloud bottom. To solve these problems, three-dimensional measurements of cloud are indispensable. Also, to estimate the calculated radiative fluxes at the TOA, spectrally integrated fluxes are not powerful to examine the role of respective components in the atmosphere, such as water vapor, aerosols and clouds, to the radiation, and it is necessary to have the spectral distribution of radiative fluxes.

Basically, the radiation budget at the TOA and the surface should be estimated by calculation with atmospheric parameters including cloud parameters.

Table 3. Scientific requirements for radiation budget

parameters	resolution/accuracy	remarks
cloud amount	0.05	
cloud bottom height	100 m 100 m	
optical thickness of cloud	0.1 (<10), 1.0 (<100)	
cloud phase	water/ice	
effective radius of cloud droplet	<2 $\mu$ m	
liquid water content	0.01g/m <sup>3</sup> or 10g/m <sup>2</sup>	
ice water content	0.001g/m <sup>3</sup> or 1g/m <sup>2</sup>	1/10 of LWC
downward shortwave flux(SFC)	< 10W/m <sup>2</sup>	
downward longwave flux(SFC)	< 10W/m <sup>2</sup>	
downward total flux(SFC)	< 20W/m <sup>2</sup>	
shortwave absorption(TOA)	< 10W/m <sup>2</sup>	
outgoing longwave radiation(TOA)	< 10W/m <sup>2</sup>	spectra should be required
surface albedo	3%	
surface emissivity	???	
temperature profile	$\pm$ 1deg	
humidity profile	$\pm$ 5%	
resolution: horizontal vertical	100 x 100 km <sup>2</sup> 0.3km	
Observation duration	2yrs + 1yr if available	

### 3.4. Polar cloud and radiation

Polar cloud climatology is an urgent issue to be solved for the study of global radiation budget, since the cloud radiative effect is very special in the polar regions. However, observation of clouds in the polar regions from passive sensor data, visible, infrared or microwave, involves many difficulties on account of the high albedo, low temperature and high emissivity of the snow and ice covered surfaces. High altitude of the ice sheet surface in Greenland and Antarctica, strong surface temperature inversion near the surface in both polar regions and various surface condition of the sea ice make the problem more difficult. The ice crystal precipitation dominated in the boundary layer of polar atmosphere is another components make it difficult to distinguish between clear and cloudy atmosphere. Cloud-radiation-ice interaction is to be solved for the radiation budget at the surface.

If the vertical structure of clouds is retrieved, it might become possible to compile the cloud climatology and radiation budget more precisely. Some clouds in polar regions over snow and ice surfaces, where it had been difficult to detect by visible and infrared imageries, will be easily detectable. Cloud radar and lidar make it possible to measure the vertical distribution of clouds over the ice surface as well as over the sea and land. Therefore it is expected to obtain global three-dimensional distribution of clouds. Reliable detection of clouds, scene identification, is essential

to estimate radiative fluxes at the TOA through BRDF from radiance measurements and then for the earth radiation budget study. Vertical distribution of clouds controls the distribution of atmospheric radiation budget, and especially the bottom of clouds affects the surface radiation budget.

Spectral longwave radiation measurements using FTIR are also indispensable especially in the 400 - 600  $\text{cm}^{-1}$  wave number region. Spectral radiation measurements at the top of the atmosphere have strong information on the vertical distribution of the atmospheric temperature and components. In the polar regions, due to extremely low amount of water vapor, absorption in the water vapor rotation band is not saturated and window in 500  $\text{cm}^{-1}$  region opens ("Arctic window"). Since the surface temperature is very low in the polar regions, the Planck Function of the black body radiation peaks in this wave number region and then upward radiation is strongly affected by the performance of this window. Not only the downward radiation at the surface, but also vertical distribution of radiative cooling is also affected by this wave number regions (Stamnes et al., 1999).

### 3.5. 3-Dimensional distribution of cloud and aerosol

Current problem:

Global distribution of aerosols is one of the most unknown parameters, especially over land because of its difficulties of satellite derivation using passive sensors. Aerosols in the polar regions are especially difficult to detect. Also, the most part of aerosols come from land areas as natural and artificial sources. So aerosols over land should be observed.

On the other hand, there are several heavy aerosol sources over the globe such as yellow sand, Saharan desert for dust particles and tropical forest fires for carbonaceous aerosols. These aerosols may be transported and diffused to the whole globe by weather systems. In order to clarify this global transportation of aerosols, vertical distribution of density and size distribution index of aerosols is required.

Table 4. Scientific requirements for mapping global aerosol distribution

parameters	resolution/accuracy	remarks
Optical thickness of aerosol	0.05 at 0.5 $\mu\text{m}$	instantaneously
Angstrom exponent	0.1	horizontally and vertically
spatial resolution: horizontal vertical	100 x 100 $\text{km}^2$ 0.3km	statistically
time resolution	TBD (5 to 10 days composite ?)	statistically

### 3.6. Cloud-aerosol interaction

As pointed out by Section 2.1.2, the climate forcing of the cloud-aerosol interaction process should be clarified for improving our prediction ability of global warming phenomenon. It is highly necessary to monitor global distributions of aerosol optical thickness, types, cloud optical thickness, effective particle radius, and precipitation. Investigation of correlation among these parameters is useful for global modeling of cloud-aerosol interaction phenomenon. Investigation of precipitation and drizzle particle amount as a function of aerosol loading is a challenging but attractive subject for the study. In order to attain these tasks, combination of imager, CPR, and lidar is needed.

Table 5 gives required accuracy/resolution of these parameters from satellite remote sensing. Our preliminary study with passive remote sensing methods has shown a positive linear correlation between cloud optical thickness and logarithm of the columnar aerosol particle number,  $\log_{10}(N_a)$ , and also a negative linear correlation between effective particle radius and  $\log_{10}(N_a)$ , without a noticeable change in the cloud liquid water path. Investigating the correlation chart of the preliminary study, it is found that the effective particle radius has to be obtained with an accuracy of 1  $\mu\text{m}$  in order to have a confidence in the obtained correlation. Also, it should be noted that the observed difference between ocean and land is about 2.5  $\mu\text{m}$  (Han et al., 1994; Kawamoto et al., 2000). Expected change in the cloud optical thickness with a change of 1  $\mu\text{m}$  in the effective particle radius is about 1, under the assumption of insignificant change in the cloud liquid water path. Vertical distribution of the effective particle radius and optical thickness classified with cloud top height will be another useful information. Since the radar signal is strongly dependent on large particles, a retrieval of drizzle amount as a function of altitude is also possible.

Aerosol information is indispensable for the study of cloud-aerosol interaction phenomenon. A key parameter for the study is the aerosol particle number, but this parameter cannot be observed from space directly and has to be evaluated from other observables from satellites. Important parameters for this evaluation are optical thickness and Ångström exponent. Since the dependence of cloud parameters on the aerosol particle number is with logarithmic one, the aerosol optical thickness has to be retrieved with a relative error less than 10 %, and the Ångström parameter has to be obtained with an accuracy of 0.2. Even with such aerosol parameters, the obtained columnar aerosol particle number can have an error of factor of 10. Such error can be caused from a wrong assumption of the aerosol size distribution, such as error in the assumed dispersion of the size distribution. It is useful, therefore, to guess the aerosol

useful, therefore, to guess the aerosol type, such as sulfate, carbonaceous, mineral-dust and sea-salt, from satellite remote sensing and/or aerosol transport modeling in order to guess the shape of aerosol size distribution.

The characteristic spatial scale of the cloud change due to cloud-aerosol interaction is of order of several hundred kilometers, so that the spatial resolution of retrievals should be of order of 100km square. Vertical resolution should be less than several hundred meters, taking into account that the height of dense aerosol layer is of 1km. One month statistics should be obtained for the correlation study, because of large variability of the parameters involved in the analysis. Morphological studies of cloud pattern such as ship trail clouds (Coakley et al., 1987) will be useful for detecting the phenomenon.

Table 5. Scientific requirements for estimating cloud-aerosol interaction

Parameters	Resolution/accuracy	Remarks
Optical thickness of cloud	1	Classified with cloud type
effective radius of cloud	1 $\mu\text{m}$	Vertical distribution needed
optical thickness of aerosol	0.1 in $\log_{10}(\tau_a)$	$\lambda = 500\text{nm}$
Ångström exponent of aerosols	0.2	Aerosol type is useful
resolution: horizontal vertical	100 x 100 $\text{km}^2$ 0.2km	Monthly average
observation duration	2yrs + 1yr if available	

### 3.7. Summary

A summary of scientific requirements is presented in the following table. The column 4, "obs/ calc/ data" in the table means each item of requirements(column 2) can be estimated by observation(obs), calculation(calc) or other data base(data).

Table 6. Summary of requirements

	requirements	resolution/accuracy	obs/ calc/ data	remarks
Aerosol (cloud-aerosol interaction)	optical thickness	0.1 in $\log_{10}(\tau_a)$	obs	
	Angstrom index	0.2	obs	
	horizontal resolution	100 km x 100 km		
	vertical resolution	0.2 km		
	time resolution	TBD		
Aerosol (Stratosphere)	optical thickness	0.05 at 500nm	obs	
	Angstrom index	0.1	obs	
	horizontal resolution	100 km x 100 km		
	vertical resolution	1 km		
	time resolution	TBD		
Cloud (GCM modeling)	cloud fraction	0.05-0.1	obs	
	optical thickness	$\Delta\tau/\tau = 0.5 - 1$	obs	
	ice water content	TBD		
	size distribution index			
	cloud top/bottom		obs	
	horizontal resolution	100 km x 100 km		
	vertical resolution	0.3 km		
Cloud (Radiation budget)	cloud type	Stratiform/convective		
	cloud fraction	0.1	obs	
	optical thickness	1	obs	
	cloud phase	water/ice	obs	
	effective radius of cloud particles	2 $\mu\text{m}$	obs	
	ice water content	0.001g/m <sup>3</sup> or 1g/m <sup>2</sup>	obs	
	liquid water content	0.01g/m <sup>3</sup> or 10g/m <sup>2</sup>	obs	
	size distribution index	TBD		
	cloud top/bottom	100 m / 500 m	obs	
	horizontal resolution	100 km x 100 km		
	vertical resolution	0.3 km		
	time resolution	TBD		
	Cloud (Conversion rate)	cloud water / ice content	< 0.2g /kg	obs
cloud top / bottom temperature		<1 K	obs	
horizontal resolution		1 km x 1 km		
vertical resolution		< 0.5 km		
time resolution		TBD		

Table 6. (Continued)

	requirements	resolution/accuracy	obs/ calc/ data	remarks
Radiation budget	downward shortwave flux(SFC)	< 10W/m <sup>2</sup>	calc	
	downward longwave flux(SFC)	< 10W/m <sup>2</sup>	calc	
	downward total flux(SFC)	< 20W/m <sup>2</sup>	calc	
	shortwave absorption(TOA)	< 10W/m <sup>2</sup>	calc	
	outgoing longwave radiation(TOA)	< 10W/m <sup>2</sup>	calc	
	surface albedo	3%	obs	
	surface emissivity	?	data base	
Temperature profile			obs data base	
	horizontal resolution	100 km x 100 km		
	vertical resolution	0.3km		
	time resolution	TBD		
	accuracy	± 1K		
Water vapor profile			obs data base	
	horizontal resolution	100 km x 100 km		
	vertical resolution	0.3km		
	time resolution	TBD		
	accuracy	± 5%		

## 4. Mission Scenario

### 4.1. Sensors

#### 4.1.1. Cloud profiling Radar(CPR)

##### (1) General Description

Cloud profiling radar (CPR) is a sensor which measures radar backscattering from cloud particles and is capable of measuring three-dimensional distribution of clouds. CPR needs much higher sensitivity to detect clouds than conventional weather radars for rain measurements. Large difference in the sensitivity required comes from difference in target size between cloud particles and rain droplets. To realize high sensitivity radar, millimeter wave frequency of 94 GHz is used for CPR. The 94 GHz radar has 39 dB higher sensitivity inherently to cloud particles than 10 GHz radar does (Rayleigh gain) under the same radar system parameters but for different frequency.

The 94 GHz frequency band, located in near center of an atmospheric window, is one of optimum frequency bands for CPR because of both relatively small attenuation incurred from atmospheric gasses and high enough frequency. We have difficulty in building CPR at further higher frequency because of immaturity of the technology and increase in atmospheric loss. New frequency allocation for satellite-borne cloud radar was approved for frequency band between 94.0 GHz and 94.1 GHz in the WRC-97 Meeting 1997 under ITU. However, consideration is requested in the satelliteborne CPR operation to protect radio astronomy observation which is carried out in nearby millimeter frequency bands.

Advantages of CPR over other remote sensors for cloud measurement from space are:

- i) Global three-dimensional cloud distribution is obtained. Cloud water (ice) content profile is estimated quantitatively by using relation between radar backscatter intensity and these quantities.
- ii) Cloud base height can be detected for most clouds owing to range resolution capability of the radar and much smaller attenuation expected than that for lidar. Cloud base height is the key information to deduce the radiation budget at the surface.

The baseline characteristics of satelliteborne CPR is i) high sensitivity to detect most clouds playing significant roles in radiation; ii) non-scanning and looking only in nadir; iii) cloud backscatter power is obtained.

The baseline design of CPR proposed so far is useful for research of cloud

radiation statistics. In the Atmos-B1 program, more emphasis is put on process study of cloud-radiation-aerosol interaction in addition to statistical study. For this purpose, an enhanced multi-function CPR is proposed based on recent design study. Finite observation width in cross track direction and Doppler capability can be added in the multi-functional CPR. Finite width observation in cross-track direction is realized by multi-beam antenna technology, which enables us real three-dimensional observation of clouds useful to cloud modeling. Doppler capability brings information discriminating cloud and drizzle. Feasibility of these new functions depends on satellite allowable resource. If full function is not allowed, descoped design CPR with single beam and Doppler function will be pursued.

## (2) Design consideration of multi-function CPR

Major features in the new CPR design and development are:

- (i) Observation at fixed 5 beam angles centered at nadir. Total observation width is about 40 km on the ground with 10 km beam separation.
- (ii) Doppler capability of about 1 m/s vertical velocity sensitivity.
- (iii) The target sensitivity is -32 dBZ or -36 dBZ (high sensitivity mode) to detect all clouds significant to the earth radiation budget. Where,  $Z$  is the radar reflectivity factor.
- (iv) The radar operates as a simple short pulse mode as well as an additional pulse-compression mode for higher sensitivity.

### Multi-beam capability

To realize finite width measurement in cross-track direction, antenna pointing is switched to five beam angles whose center is in nadir direction. Total observation width is 40 km in cross track with 10 km separation on the ground. Because a footprint is about 800 m in diameter on the ground, measurement area is not covered contiguous. Beam angle switching is made pulse by pulse and pulse integration is carried out at five footprints in parallel. Further increase in measurement width and improved sensitivity is being studied.

### Doppler capabilities

Nadir pointing beam has Doppler capability to detect movement with less than 1 m/s resolution in vertical direction. To maintain the correlation during consecutive two radar pulses under high ground speed in satellite observation, pulse pair interval should be very small. A possible solution to this problem is using orthogonal two polarizations for the pair pulses and enabling us to discriminate the two signals even

they are overlapped in time.

### Radar Sensitivity

The sensitivity required for CPR has been considered as -30 dBZ (IGPO, 1994). Since then, importance in high altitude cirrus for radiation budget has been suggested and further higher sensitivity is desired. The radar reflectivity factor in relation to the ice water content (IWC) is estimated for several particle sizes in Fig. 11-1 and the same but for liquid water cloud is described in Fig. 11-2. For high level cloud, the situation becomes better; the sensitivity of -32 dBZ detects 90 % of the high level clouds and further the sensitivity of -36 dBZ improves up to 93 % of detection. The field measurement results also suggest the 16 % of ice clouds are missed in the observation with -30 dBZ sensitivity. Considering these suggestions, our target sensitivity is set at -36 dBZ. Ongoing airborne CPR experiments will help evaluate the target sensitivity needed in the satellite CPR measurement. The relation between the radar reflectivity factor and cloud particle size is shown in Fig. 11-2.

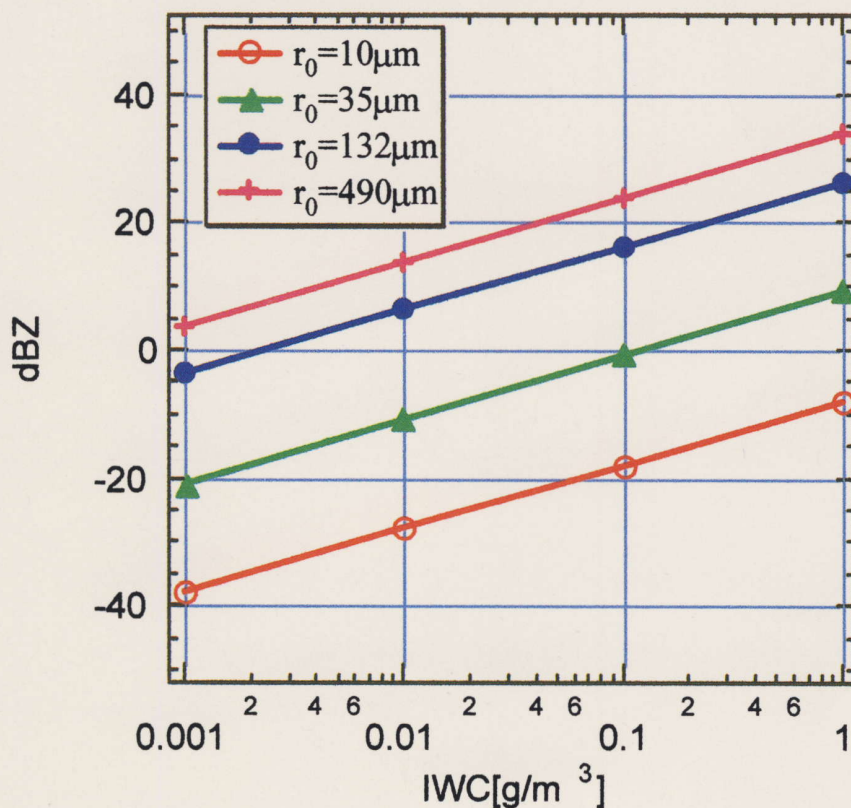


Fig. 11-1. The relationship between the radar reflectivity factor Z and ice water content IWC for given size of ice crystals.

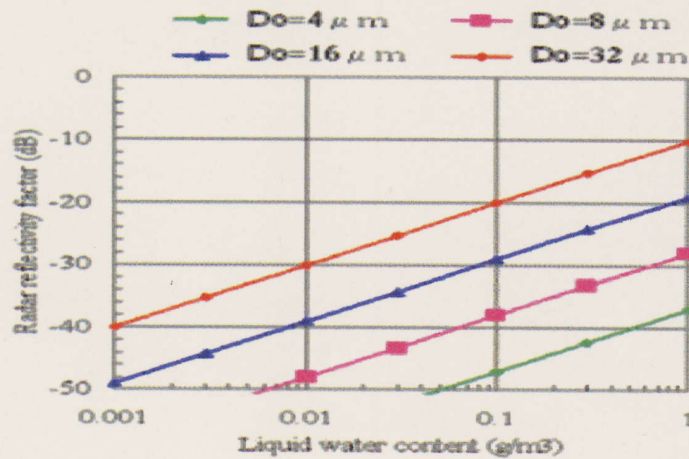


Fig. 11-2. The same as Fig11-1 but for water clouds.

Concerning cirrus clouds and when we take the reported values for the IWC to be  $0.001\text{gm}^{-3}$  with  $10\text{micrometers}$  size as a lowest ones (e.g., Dowling and Radke 1990), the requirement of the sensitivity of radar reflectivity factor can be estimated to be  $-40\text{dBZ}$ . For the same size but with IWC to be  $0.01\text{gm}^{-3}$ , the sensitivity increases up to  $-30\text{dBZ}$ .

Since there is no global data set for size distributions of cloud particles obtained directly by observations and thus there are essential difficulties in estimating the requirements of the radar reflectivity factor in a statistical manner. There is a way to estimate the sensitivity by relying on the output from General Circulation Model by assuming the empirical relationship between radar reflectivity factors and IWC. Studies by using ECHAM 4 climate model have shown that the sensitivity of  $-30\text{dBZ}$  detects 70% of the clouds and the values of  $-36\text{dBZ}$  improves up to 80% of detection (Fig. 11-3) (Lemke et al., 1997).

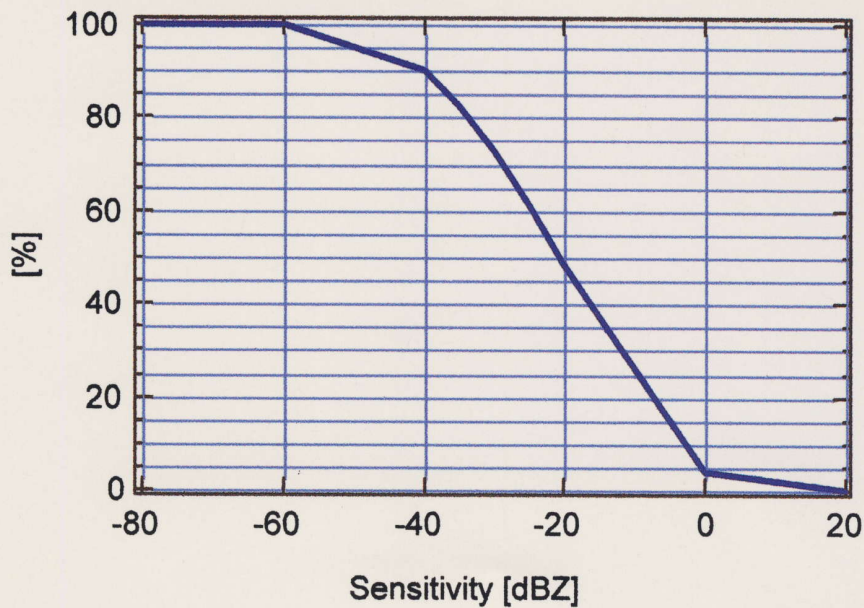


Fig. 11-3 Global distribution of apparent reflectivity derived from ECHAM 4 model out put.

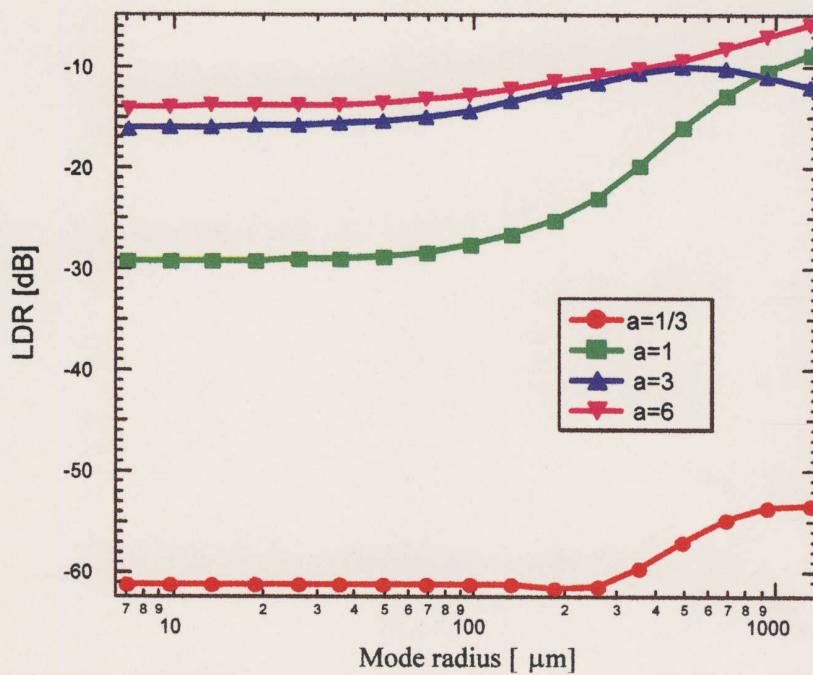


Fig. 11-4 The relationship between the linear depolarization ratio LDR and size of ice crystals. A denotes the aspect ratio of the particle and a=1/3 is the plate-like particle and a=6 is a long column.

### Designed specification

Designed specification of multifunction CPR and expected radar sensitivity are shown in Table 7 and Table 8.

Table 7. Designed specification of multifunction CPR (full function and descope function)

parameter	Full multifunction	Descope function
Frequency	94.05 GHz	94.05 GHz
Antenna size	3.1 m x 2.3 m	2.3 m (in diameter)
Antenna gain	64 dBi	65 dBi
Observation width (number of beam point)	40 km (5)	Only nadir (1)
Vertical resolution (pulse width)	500 m (3.33 us)	500 m (3.33 us)
Instantaneous footprint	800 m (-3 dB; one way)	800 m (-3 dB; one way)
Horizontal resolution	5 km	5 km
Noise equivalent Z @ 10 km height (quantity at nadir)	-17.8 (-18.2) dBZ	-21.0 dBZ
Minimum detection Z @ 10 km height (quantity at nadir)	-30.7 (-32.6) dBZ	-37.8 dBZ
Pulse repetition frequency	4500 Hz (x2)	4500 Hz (x2)
Duty ratio of EIK	< 3%	<3%
Receiver NF	5 dB	5 dB
Satellite altitude	400 km	400 km
Weight	250 kg	194 kg
Power consumption	350 W	328 W

Table 8. Assessment of expected CPR sensitivity; along track data integration for 5 km is assumed.

Altitude (km)	Full multifunction CPR (dBZ)		Descope CPR (dBZ)
	Nadir Beam (#3)	Non nadir beam (#1,2,4,5)	
2 km	-31.2	-29.2	-36.4
5 km	-32.2	-30.3	-37.4
10 km	-32.6	-30.7	-37.8

### (3) Technical Issues

One of critical components in the CPR development is millimeter wave transmitter tube (EIK: Extended Interaction Klystron) for space use because it is not existing, yet. However, design and material study conducted so far confirmed the feasibility of EIK of space use with life time more than two years. By 1999, EM of EIK for vibration test was completed and successful in the test. The development of this model was partially supported by Communications Research Laboratory. Currently, the next phase of EM is being developed. Considering these development efforts and

interim outcomes, development of EIK for the satellite use will be feasible in about three years of development phase. Other than the EIK tube, there is some technical challenge in manufacturing large-diameter millimeter wave antenna, low-loss and high-speed switching feed system, and antenna accommodation to the satellite. However, these will be solved within existing technologies.

#### (4) Technical demonstration with airborne CPR

For the purpose of demonstrating technical feasibility and usefulness of the millimeter wave CPR, an airborne CPR has been developed by Communications Research Laboratory. The first test flights were conducted in March 1998. In the airborne CPR experiment, since much higher sensitivity will be achieved compared with that of satellite-borne system, an assessment for the target sensitivity for the satellite system is being carried out and data analysis is ongoing. An example of airborne CPR is shown in Fig. 12, in which the vertical distribution of Z, Doppler velocity, Linear Depolarization Ratio (LDR) are shown in each panel. LDR is an indicator of non-sphericity of ice crystals (Okamoto et al., 1995). In Fig. 11-4, the relation between LDR and size of cloud particles is estimated. Note that spherical particle does not produce any non-zero LDR. Required sensitivity and applicability of Doppler and multiparameter functions to satellite system are being studied using experiment data. The airborne CPR system should be improved as a multiple sensor platform on which the CPR, lidar, and radiometers operate simultaneously. Along with the airborne experiment, a ground based system using the CPR together with co-located lidar and microwave radiometer has been developed. Synergy algorithm for 95GHz radar and lidar systems is currently developing for the retrieval of microphysical information such as IWC/LWC and size of particles. The airborne and ground based systems developed so far will also be used for validation of satellite observation.

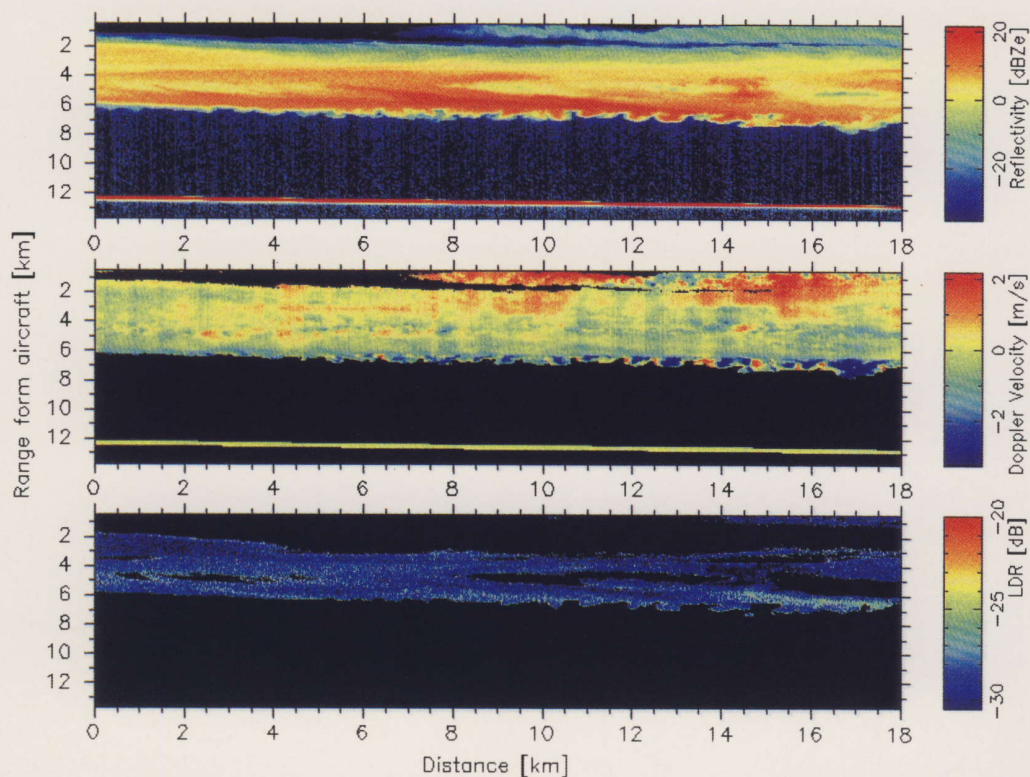


Fig.12. Vertical distribution of reflectivity (Z), Doppler velocity, Linear Depolarization Ratio (LDR) obtained from airborne CPR.

#### 4.1.2. LIDAR

##### (1) Outline of LIDAR

LIDAR or Laser Radar is a technique similar to radar. A lidar uses laser as a light source while a radar uses radio wave instead. LIDAR is an acronym of LIght Detection And Ranging, which is an analogy of RADAR or RAdio Detection and Ranging. By using light instead of radio wave, a lidar can measure distribution of clouds and even aerosols which are much smaller than cloud particles and rain drops. A lidar for measuring aerosols is called Mie scattering lidar, because the lidar detects scattering of light by a particle with its diameter comparable to wavelength of light and particle shape is approximated as a sphere, which enables us to apply Mie theory to calculate the scattering signature of the particle.

In Mie scattering lidar measurements, a laser pulse transmitted to the atmosphere is scattered by atmospheric particles such as aerosols and clouds. The light scattered backward to the lidar is collected by a telescope and detected as a function of time. The delay time between the laser emission and the detection of backscattered light corresponds to the range where the laser pulse was scattered, and the detected intensity is proportional to scattering efficiency of the particles, which can be converted to a density distribution of particles.

A Mie scattering lidar system generally consists of a laser, a transmitting optics, a receiving telescope, an optical detection system, and a data collection system. A Mie scattering lidar for measuring aerosols and clouds uses a high power laser with a wavelength which is not tuned to absorption lines by atmospheric gaseous species. Fundamental output of a Nd:YAG laser at 1064 nm and the second harmonics at 532 nm are often used.

## (2) LIDAR development status and strategy

A space-borne lidar equipment named Experimental Lidar In-Space Equipment (ELISE) has been developed by NASDA for the Mission Demonstration test Satellite-2 (MDS-2), which was originally planned for launch in 2002 for technological validation of space-borne lidar measurements in advance to the operational mission of ATMOS-B1. In the recent review of the NASDA's programs after the failure of the H-II rocket launch in November 1999, the MDS-2 program was canceled. However, the development and the ground-based test of ELISE are being continued to establish the technology. The specifications for ELISE were defined by NASDA based on the study conducted by the National Institute for Environmental Studies (NIES) (Sasano and Kobayashi, 1995). ELISE is a two wavelength lidar employing fundamental and second harmonics of a Nd:YLF laser (1053 nm and 527 nm). ELISE has three receiver channels: An analogue detection channel and a photon counting channel at 1053 nm, and a photoncounting channels at 527 nm. The analogue channel is operated in the daytime and nighttime, and the photon counting channels are operated only in the nighttime. The parameters for ELISE are listed in the left column of Table 9.

The study of the ELISE data analysis and data utilization has been conducted by NIES in the research cooperation between NIES and NASDA. A detailed simulation of measurements with ELISE was carried out (Liu, Voelger and Sugimoto, 2000). It was shown from the computer simulation that cloud top altitude and thickness of cirrus, top of cloud below the cirrus, and the ground surface can be measured with analogue channel at 1053 nm either in the daytime or the nighttime. Possibility of measuring

bottoms of lowerclouds depends on optical thickness of the clouds. Aerosols in atmospheric boundary layers, and dust layers such as Asian dust (Yellow sand) can be observed with 1053 nm analogue channel and with photoncounting channels at both wavelengths when the signal-to-noise ratio is improved with a reduced horizontal resolution. Stratospheric aerosols after major volcanic eruptions can also be measured with a reduced horizontal resolution in the nighttime, and that can provide useful information on transport of stratospheric aerosols and general circulation. Also, polar stratospheric clouds can be observed with ELISE.

A simulation study including multiple scattering was also carried out with the Monte Carlo method (Voelger, Liu and Sugimoto, 1999). The result shows that the multiple scattering effect is larger for larger particles, however the dependence of the effect on the receiver field-of-view (FOV) is larger for smaller particles where sideward scattering is larger. The method for correcting the multiple scattering effect in the data reduction is also being studied.

The Mie scattering lidar for ATMOS-B1 (tentatively named ELISE2) is being designed on the technical achievement of ELISE so that it can operate for three year mission period. Tentative parameters for ELISE2 are listed in the right column of Table 9. A depolarization channel is added at 1053 nm for depolarization ratio measurement to estimate proportion of ice to water droplet in cloud. Both 1053-nm and 527-nm channels will be operated in analogue mode continuously in the daytime and nighttime with a high horizontal resolution.

Table 9. Parameters for ELISE and ELISE2

	ELISE	ELISE2
Orbital altitude	550 km	380 km
laser wavelength	1053 nm and 527 nm	1053 nm and 527 nm
laser output power	77 mJ/pulse at 1053 nm	80 mJ/pulse at 1053 nm
	9 mJ/pulse at 527 nm	9 mJ/pulse at 527 nm
pulse frequency	100 pulse/sec	35 pulse/sec
laser beam divergence	0.17 mrad	0.25 mrad
receiver telescope diameter	1000mm	1000 mm
receiver field of view	0.22 mrad	0.3 mrad (TBD for the wide FOV channel)
receiver channel/detector	1053 nm analogue (AN)/APD*	1053 nm AN/APD
	1053 nm photoncounting (PC)/APD	1053 nm depolarization AN/APD
	527 nm photoncounting (PC)/APD	527 nm AN/PMT**
		527 nm Wide FOV (Ring FOV) AN/PMT
efficiency of receiving optics	0.4 (1053 nm analogue)	0.4 (1053 nm P-polarization)
	0.05 (1053 nm photoncounting)	0.4 (1053 nm S-polarization)
	0.6 (527 nm photoncounting)	0.4 (527 nm)
filter bandwidth	0.3 nm (analogue channel)	0.1 nm (for 527 nm)
	4 nm (photon counting)	0.3 nm (for 1053 nm)
quantum efficiency	0.45 (1053 nm analogue)	0.45 (1053 nm P-polarization)
	0.0125 (1053 nm photoncounting)	0.45 (1053 nm S-polarization)
	0.34 (527 nm photoncounting)	0.1 (527 nm)
vertical resolution	100 m	100 m
number of data accumulations	20	1
horizontal resolution	1.5 km	200 m
Weight	250 kg	TBD
Power	630W (at the peak)	TBD

\*APD: Avalanche photodiode, \*\*PMT: Photomultiplier tube

Results of the simulation for ELISE2 using parameters in Table 9 are shown in Fig. 13 and Fig. 14. The results show that ELISE2 will provide with useful data on clouds and aerosols at the two wavelengths. To improve the performance in the daytime observation at 527 nm, the development of a narrow band interference filter is required. The addition of the wide FOV (ring FOV) channel should be considered for ELISE2. From the results of the Monte Carlo simulation carried out for ELISE, the two receiver channels with different FOVs will be useful for categorizing aerosol types and characterizing clouds.

### (3) Future studies

The following issues concerning data reduction algorithms and data utilization methods are currently conducted for ELISE:

- establishment of an observation strategy for effective data acquisition for use in cloud climatology (statistical analysis), aerosol climatology and in cloud physics,
- effectiveness of lidar data use in improvement of climate prediction models,
- data processing algorithms including calibration, quantitative analysis, multiple scattering correction, and use of two-wavelength lidar data.

Further investigation are required for ATMOS-B1 lidar on

- hardware study to meet the resource requirements,
- depolarization and multiple scattering characteristics,
- synergism with other sensors.

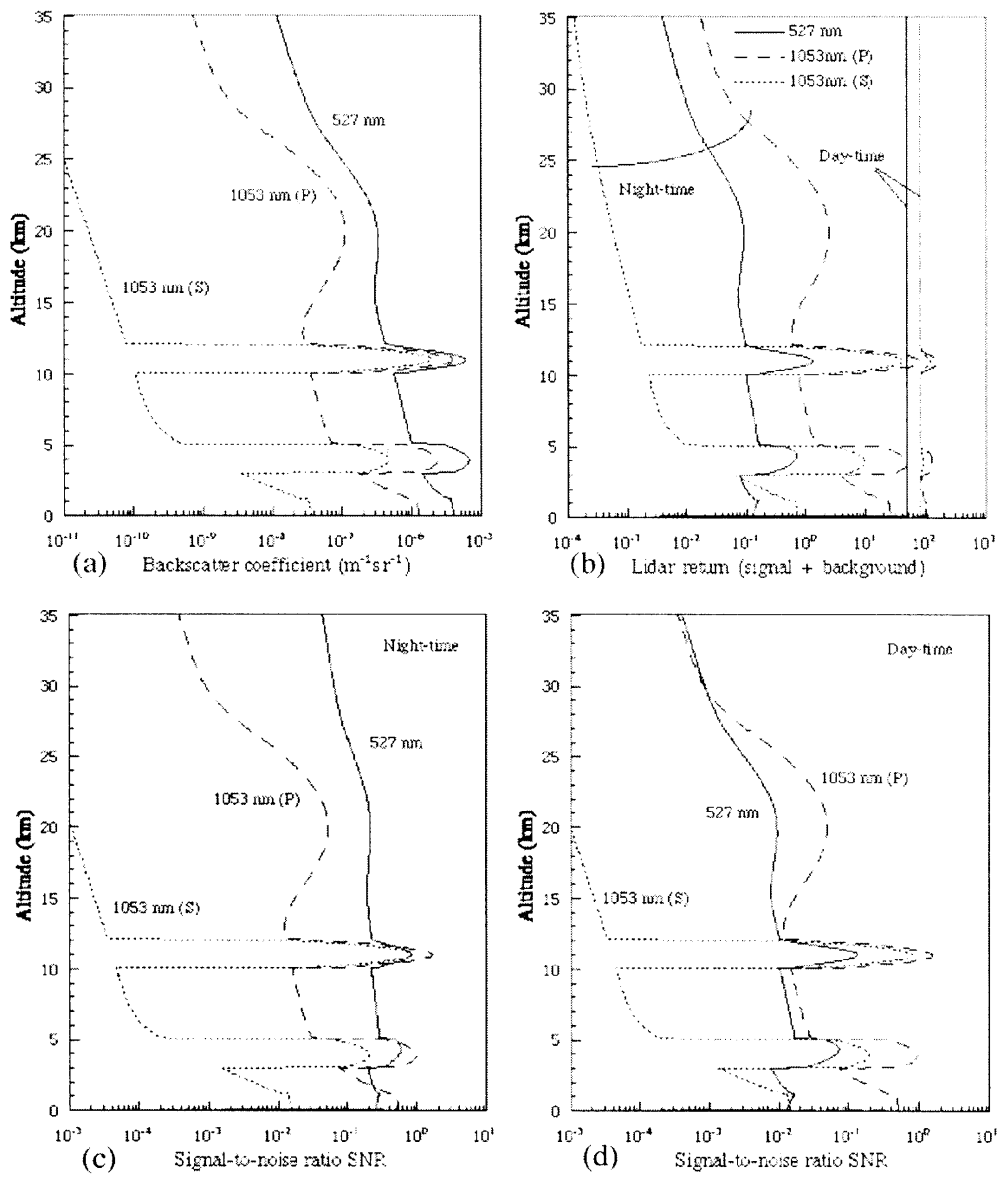


Fig. 13. Results of the simulation for ELISE2. (a) modeled backscatter coefficient, (b) simulated lidar signal (photoelectron number) for a single-shot measurement, (c) single-shot signal-to-noise ratio (SNR) in the nighttime, and (d) SNR in the daytime.

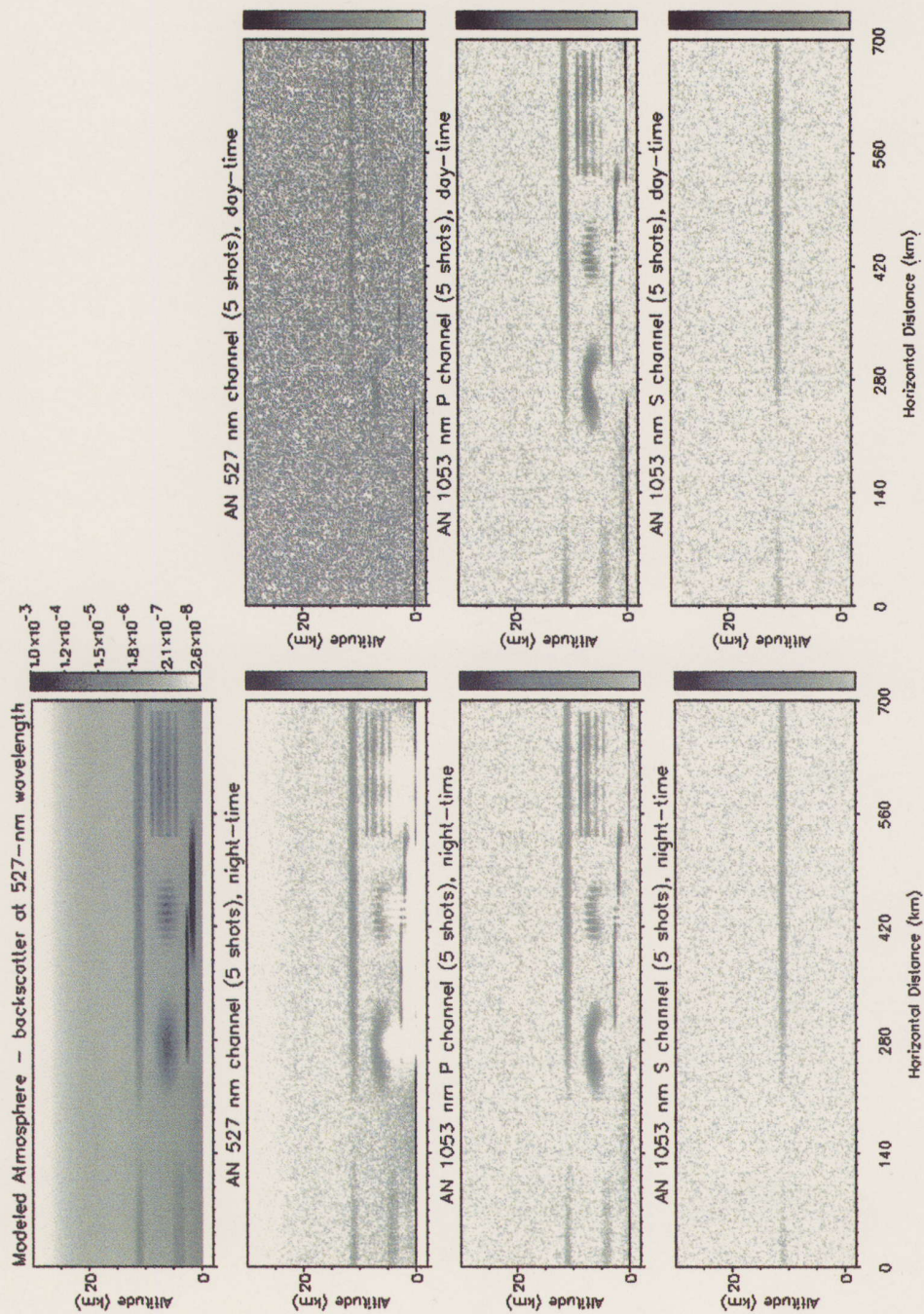


Fig.14. Simulation of observation with ELISE2. Modeled clouds and aerosols (uppermost left), simulated nighttime data (left panels) and daytime data (right panels) for the three detection channels. Number of accumulation is 5 (1-km horizontal resolution).

#### 4.1.3. Imager for cloud mapping

Since measurements performed by CPR and lidar, as major sensors used for this mission, are limited to narrow lineal sections, a visible/infrared imager is required to observe the global distribution complementarily. Remote sensing technique using space-borne visible/infrared radiometer has been developed mainly with the NOAA/AVHRR and the similar sensors, which has been almost established. Optical thickness, effective particle radius, and integrated water amounts of clouds, can be estimated through visible and near infrared wavelengths with reflected solar radiation measurements (Nakajima and King 1990). On the other hand, cloud top temperatures (or altitude) can be also estimated by observing infrared radiation emitted from the cloud surface (Rossow and Schiffer 1991). Optical thickness and effective particle radius of cirrus clouds, which cannot be measured by above techniques, can be estimated by the split window technique (King et al. 1992). Cloud amount for some representative levels, is comprehensively estimated from the optical and microphysical characteristics retrieved from the imager (Rossow and Schiffer 1991) as well as the cloud top and base height using CPR and lidar. Based on the results of these observations, the radiation budget is obtained at the top of the atmosphere and at the surface. Near infrared information will provide the discrimination of cloud particles whether ice or water (Crane and Anderson 1984, Liou 1992) and the identification of cloud over snow surfaces (Crane and Anderson 1984). Middle infrared will also enable us to identify cloud over snow and ice surfaces (Score 1989, Yamanouchi and Kawaguchi 1992).

In this mission, it is presumed that sensors such as NOAA/AVHRR or TRMM/VIRS etc are most suitable as a cloud imager. But it is possible to make the concurrent observation with other satellite sensors due to limitation of the weight and power demand of the entire satellite. Required fundamental specifications should include: (1) three channels for the visible to near-infrared range and three channels for the middle to thermal infrared range, (2) spatial resolution of 1 km or less, (3) scanning width of 1,000 km and (4) 10 or more bits dynamic range. It is better that they can be calibrated for each wavelength after launch. Required wavelengths of visible/infrared radiometers and the corresponding cloud parameters to be observed, are simply summarized in the table 10.

Table 10. Visible Infrared Radiometer and Items of Observation

Wavelength ( $\mu\text{m}$ )	Items of Observation
0.63	Optical thickness of cloud
1.6	Discrimination of cloud thermodynamic phase whether ice or water; identification of cloud over snow surfaces
2.2	Effective radius of cloud particles
3.75	Effective radius of cloud particles; identification of cloud over snow and ice surfaces
10.8	Cloud top temperature; optical thickness and effective particle radius of cirrus cloud
12.0	Cloud top temperature; optical thickness and effective particle radius of cirrus cloud
spatial resolution	1 km or less
swath	1000 km
dynamic range	10 bits or more

If sun-synchronous orbit is adopted, it is possible to monitor the cloud - water cycle in particular over the polar region, which is impossible for geostationary satellite only.

#### 4.1.4. FTIR

The objective of this mission is to clarify a radiative process of cloud and aerosol and to improve the estimation accuracy on radiation budget at the TOA and the surface, which cannot be directly observed by passive sensors. In this program, radiation budget from the top to the surface will be estimated by numerical calculation using atmospheric and surface parameters, some of which are observed directly and indirectly, and others are derived or assimilated from other satellite or ground-based observation data. FTIR spectrometer can give the thermal spectra emitted from the earth-atmosphere system. These spectra can reflect some details of atmospheric radiation processes including clouds, aerosols and gases.

Vertical profiles of temperature and humidity, which are indispensable for radiation estimation, can be derived from these spectra. Also, emissivity for infrared region and effective radius of ice crystals of cloud can be estimated.

The specification of the FTIR spectrometer should have spectral resolution less than  $1\text{cm}^{-1}$  between  $600$  and  $1500\text{cm}^{-1}$  to achieve an accuracy of retrieved temperature and humidity with standard deviation of 1 degree and 10% theoretically. The spatial resolution is required to be smaller as possible in order to avoid the non-uniform cloud effect.

Since the success of ADEOS/IMG, there are many on-going satellite FTS programs, such as ENVISAT/MIPAS, METOP/IASI, Chem/TES, SciSAT/ACE,

GCOM-A1/SOFIS, GHIS, etc. ATMOS-B1/FTS instrument has heritage of IMG, but it has more similarity to IASI and GHIS. Currently, the specifications of the ATMOS-B1/FTS (Table 11) are under discussion for three major topics, 1) Spectral coverage, 2) Spectral resolution, and 3) Data rate and/or footprint interval.

Minimum requirement for the spectral coverage is currently 600 to 1800  $\text{cm}^{-1}$ , which is based upon the limit of Photo-Volatic (PV) type MCT(HgCdTe) detector. But, there is strong requirement to extend longer wavelength edge down to 400  $\text{cm}^{-1}$ , or 25  $\mu\text{m}$  to observe emission of  $\text{H}_2\text{O}$  rotational lines which is believed to be a significant source of error on earth radiation budget (Fig. 15). The REFIR, an FTS proposal to ESA in phase A, which was originally a part of ERM proposal, is claiming that the observation down to 100  $\mu\text{m}$  should be necessary. To extend the spectral coverage, it is necessary to add another detector, which increase the complexity and cost of the FTS. The PV-MCT detector shows very good linearity which is essential for the accurate temperature retrieval. Past programs, such as IMG, used PC-type MCT detector where the non-linearity issue was very difficult to correct properly. Several other advantages of PV-MCT detector are high impedance, low heat production, and low 1/f noise.

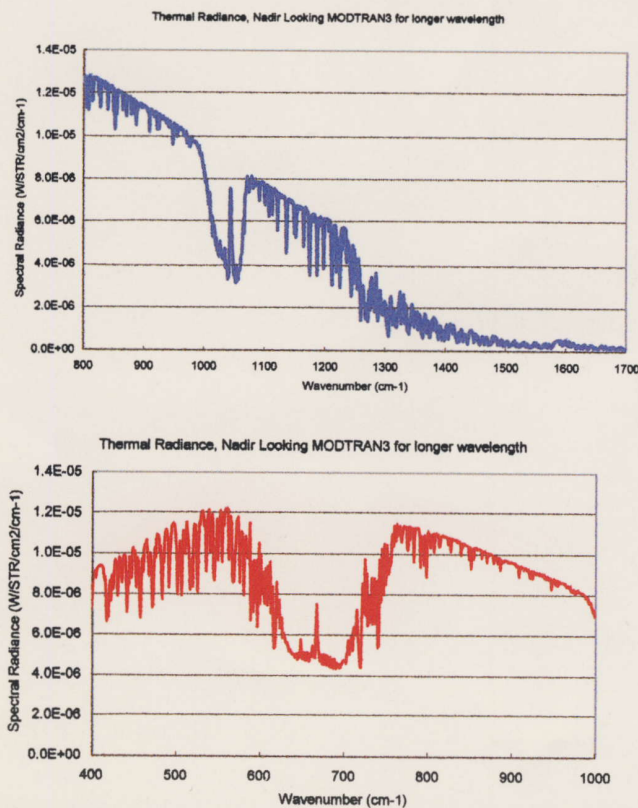


Fig. 15. Thermal emission to be observed at the top of atmosphere, calculated by MODTRAN3

Spectral resolution of the Michelson interferometer has strong relation to 1) size of instrument, 2) scan interval, and 3) data rate. The  $1.0 \text{ cm}^{-1}$  spectral resolution should be enough for temperature and water vapor retrieval. Higher spectral resolution,  $0.1 \text{ cm}^{-1}$ , as demonstrated in IMG experiment can give vertical profiling of several other chemical species and better vertical resolution of temperature and water vapor.

Footprint interval determines the interferogram sample interval, which is inversely proportional to the data rate. Fig. 16 demonstrates rough relationship between footprint interval and data rate. An  $8 \times 1$  pixels linear imaging FTS will require very high data rate,  $180 \text{ kbp} \times 8 = 1.4 \text{ M bps}$ , even at  $1 \text{ cm}^{-1}$  spectral resolution. Thus, non-imaging NADIR observation is assumed for the specification.

A dual pendulum design FTS based upon commercial laboratory model (BOMEM MR-200) was tried for vibration test during the concept study of solar occultation FTS for space station funded by NASDA. It showed very good feasibility for the H-II launching environment, and the base model (MR-200) has already flight proven under zero gravity. There should be trade-off between this dual pendulum design and linear motor design similar to the IMG. The dual pendulum design should show smaller size for the  $1.0 \text{ cm}^{-1}$  spectral resolution. But, the linear motor design of IMG was already designed, tested, flight proven, and should show superior performance for the ATMOS-B1 mission. There will be very little difference in actual development cost between IMG class,  $0.1 \text{ cm}^{-1}$ , instrument and the  $1.0 \text{ cm}^{-1}$  instrument. Table 12 compares characteristics of two classes of FTS designs, with  $0.1$  and  $1.0 \text{ cm}^{-1}$  spectral resolutions

Table 11. Minimum specification of FTIR radiometer

Number of spectral bands	1	Low SNR at high frequency region
Spectral resolution	$1.0 \text{ cm}^{-1}$	$0.5 \text{ cm}^{-1}$ unapodized
Frequency Coverage	$600 - 1800 \text{ cm}^{-1}$	$5.6 - 16.7 \mu\text{m}$
Detector	PV MCT detector	
I FOV	Nadir	
Spatial resolution	4 km	4 km circle (4 km x 4 km)
Footprint interval	50 km	About 7 sec for double side interferogram
Data rate	30 k bps	
Note	Image Motion Compensation is necessary.	For both Satellite velocity and Earth rotation

Table 12. Comparison of 0.1 cm<sup>-1</sup> and 1.0 cm<sup>-1</sup> FTS design.

	1.0 cm <sup>-1</sup> class FTS	IMG class FTS
Spectral Resolution	1.0 cm <sup>-1</sup>	0.1 cm <sup>-1</sup>
IFOV	4 km	4 km
Beam diameter	2.5 cm	10 cm
Minimum footprint interval	8 km	30 km
Interferogram acquisition	1 sec (or less)	3 sec (+ 1 sec time lag)
Relative SNR to the ch3 of IMG	1/3	1
Number of bands	2	3
Spectral Coverage	1800-850 cm <sup>-1</sup> 850-400 cm <sup>-1</sup>	1800-1100 cm <sup>-1</sup> 1100-850 cm <sup>-1</sup> 850-400 cm <sup>-1</sup>
Data rate	180 kbps for 8 km interval 30 kbps for 50 km interval	800 kbps for 30 km interval
Weight	65 kg	160 kg
Power	116W	200 W
Vertical profiles	T, H <sub>2</sub> O, O <sub>3</sub>	T, H <sub>2</sub> O, O <sub>3</sub> , CH <sub>4</sub> , CO, N <sub>2</sub> O
Total Column	CO, CH <sub>4</sub>	HNO <sub>3</sub> , CFCs
Relative development Cost to IMG	0.7	0.7

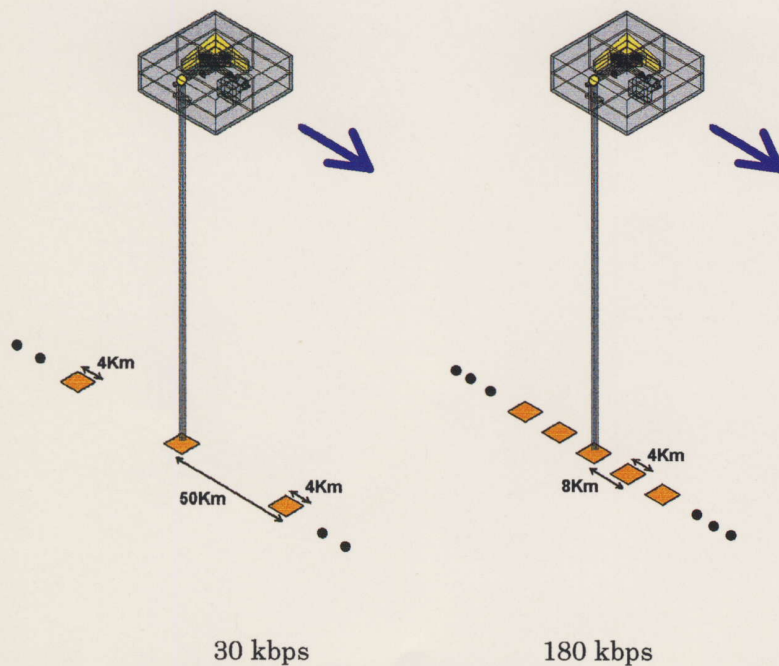


Fig. 16. Relationship between footprint interval and data rate for the 1.0 cm<sup>-1</sup> FTS. The nominal IFOV size is 4 km x 4 km, for FTS instrument at 400 km orbit. These data rate can be reduced to 1/3 by data compression.

#### 4.2. Supporting data (Ancillary data)

Since the main objective of Atmos-B1 is to examine the process of radiation in the atmosphere especially controlled by clouds and aerosols, the sensors equipped on it are very limited only to fulfill the minimum requirements. In order to meet the final mission objectives, supplementary data set from instruments on other satellites and by other meteorological analysis are needed. Though FTIR is to be equipped to supply information about the vertical profile of temperature and humidity, it is limited to clear sky area or the region above the cloud top. The data of microwave radiometers are indispensable to derive column water vapor amount and liquid water content, and the data of microwave sounders to derive temperature profile. AMSR on ADEOS-II, for example, is to provide such data.

The validation of estimated radiation budget from radiative transfer calculation based on data of cloud and aerosol profiles is to be made with the data provided by earth radiation budget instruments such as CERES, ScaRaB or ERBE. Those instruments will provide shortwave albedo, shortwave absorption and outgoing longwave radiation at the top of the atmosphere in the horizontal scale of few tens of km. Following the first flight of CERES on TRMM (Tropical Rainfall Measuring Mission), observations to cover whole globe are to be made by CERES equipped on TERRA (EOS-AM) launched on December 18, 1999.

Meteorological variables at grid points of global area will be supplied with meteorological objective analyses data. These data are basic variables to derive not only temperature and humidity profiles for the radiative transfer calculation of whole atmosphere but also indispensable to estimate cloud top and bottom temperature from backscatter lidar and cloud profiling radar. So, these data should be supplied with near real time during the basic processing of mission data. There are several kinds of data sources, such as ECMWF (European Centre for Medium Range Weather Forecasts), NCEP/NCAR (National Centers for Environmental Prediction/ National Center for Atmospheric Research), JMA (Japan Meteorological Agency), and so on.

### 4.3 Orbit

Parameters of satellite orbit must be decided to meet the mission objectives and specification of sensors onboard. Satellite altitude should be set to low around 400 km, depending on the specification of the active sensors used. For orbit inclination, various discussions have been made, but final conclusion has not been reached yet. The subject of orbit inclination will be left for the future discussion.

In the viewpoint of the importance of diurnal variations, there are ways to select solar asynchronous inclined orbits, but this is not sufficient for making global observations including the high latitude or polar region, because the regression period, important for diurnal variations, is only 60 days and maximum orbit inclination is only 55 degrees (if inclination is increased further, regression period becomes longer and observation of diurnal variation can become meaningless). Based on the importance of global observations, in particular including the high latitude or polar region, a polar orbit is desirable. In such a case, sun asynchronous becomes unnecessary and sun-synchronous polar orbit is required. Diurnal variations are not obtained, but precedence will be given to observations of the entire globe.

On the other hand, although this mission has a possibility of total radiometer, such as CERES to monitor the earth radiation budget directly and small imaging sensor, it is still important to collaborate with other satellite. If the international coordination can be made as expected, it will become possible to capture time changes in combination with other foreign satellites. Similar satellites of foreign countries are planned based on this concept.

To search the possibility of this collaboration above, the quantitative estimation of concurrent observation with other satellite sensors is needed. Some results obtained by a tentative numerical simulation on space-time sampling focused in concurrent observation with various lag time are presented here.

Two cases of orbit for ATMOS-B1 mission are presumed; one has a small recurrence period in which observation is made sparsely but quickly, the other has a longer period suitable for observing in detail but slowly. Table 13 shows orbital parameters of these two cases and that of two other satellites (EOS-AM HP 1999 Dec.; ADEOS-II HP 1999 Dec.), which are planned to carry prospective sensors. Their swath width are more than 2000km or less. Although they are not selected for simulation due to lack of complete information, NOAA/AVHRR-L-Q are of course useful and their swath width are about 3000km enough to assist ATMOS-B1 mission. The number of observation around equator and low latitude is equal to revisit capability. Therefore, the satellite revisits every 2 days or 8 days for each case, moreover in high latitude or

near polar it almost comes back quickly in case of having swath.

Table 13. Parameters of Satellite Orbits and onboard sensors

Satellite	Revisit capability (days)	Nodal Period (min.)	Inclination (degree)	Height (km)	Sensor	Swath width (km)
ATMOS-B1(1)	2	92.9032	97.091	416.72	Active	-
ATMOS-B1(2)	8	92.1600	96.9587	380.43	Active	-
TERAA	16	98.88	98.2	705	MODIS	2330
ADEOS-2	4	101	98.6	803	GLI	1600

As the required minimum difference between the arrival time of ATMOS-B1 and that of other satellite depends on the method of data analysis, three cases of time lag are presumed; 6, 15 and 30 minutes.

Fig.17 shows the ratio of occurrences of concurrent observation other satellite sensors to the whole number of observation made by ATMOS-B1 solely. Since the number of points watched by ATMOS-B1 with 2-days-cycle is less than that with 8-days-cycle, the chance of concurrent observation decreases. Therefore the ratio is 10% at most in case of 2-days-cycle as can be seen in top of Fig.17. On the other hand, the ratio increases to over 40% in case of 8-days-cycle. If the observation is required with 6-minute's time lag, the ratio may be around 10%. And the longer the time lag is, the larger the ratio is. Almost same results are obtained for both MODIS and GLI.

To achieve the aim of this mission and to be able to acquire the most meaningful data with not only ATMOS-B1 active and other sensors onboard but also with the help of other satellite sensors, further discussion is required to decide the final plan of satellite orbit.

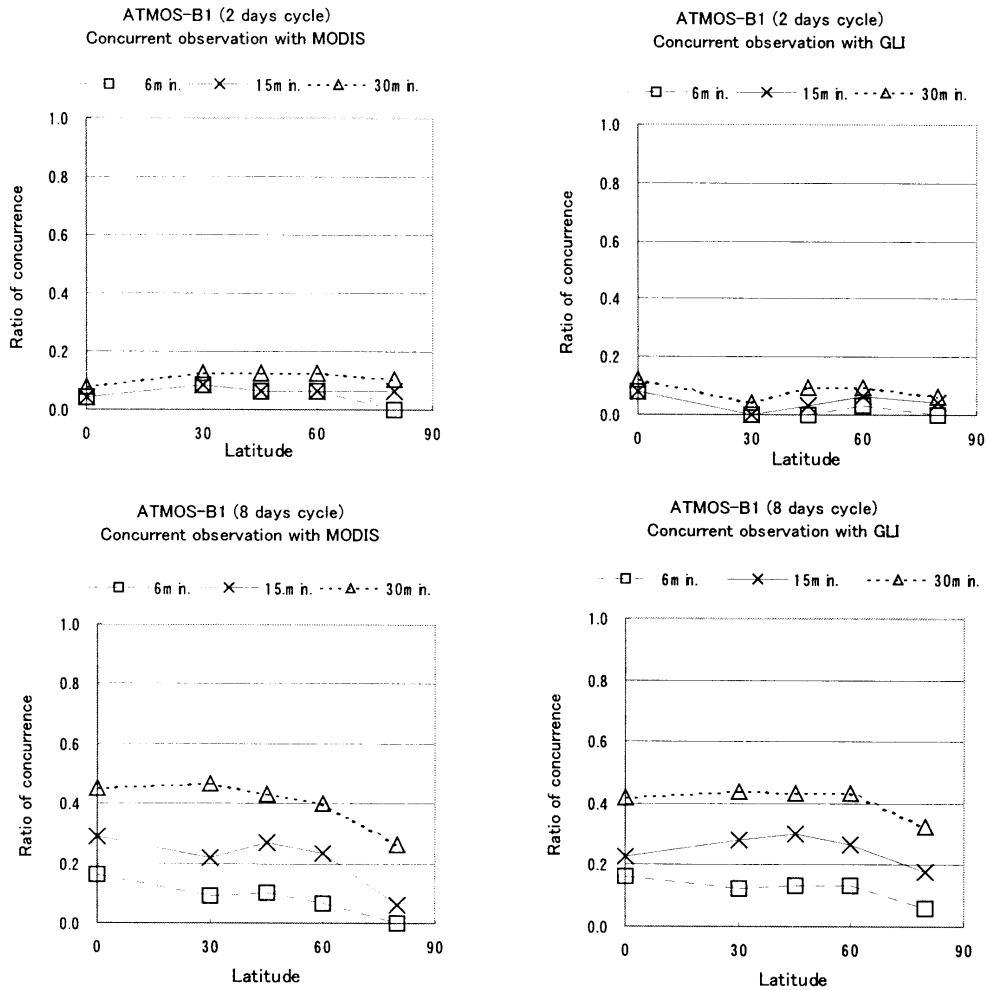


Fig.17. Possibility of concurrent observation for ATMOS-B1 with other satellite-borne sensors (MODIS (left) and GLI (right)). Three lines are ratio of the number of concurrent observation with subsidiary sensor to that of ATMOS-B1 observation for three different time lags. Two figures at top are for 2-days cycle and that at bottom for 8-days cycle. Simulation was made with following conditions; Target points are set from equator to 80 deg. in latitude and 20 degree-extent in longitude centered by epoch point. Calculated values at each sampling area are averaged in longitudinal direction. 16-days integration was performed.

## References

- Arking, A., 1964: Latitudinal distribution of cloud cover from TIROS III photographs. *Science*, 143, 569-572.
- Arking, A., 1990: The radiative effects of clouds and their impact on climate. WCRP-52.
- Chahine, M.T., R. Haskins, and E. Fetzer, 1997: Observation of the recycling rate of moisture in the atmosphere: 1988-1994. *GEWEX News*, 7, August.
- Charlson, R.J., J.E. Lovelock, M.O. Andreae, and S.G. Warren, 1987: Oceanic phytoplankton, atmospheric sulphur, cloud albedo and climate. *Nature*, 326, 655-661.
- Charlson, R.J., S.E. Schwartz, J.M. Hales, R.D. Cess, J.A. Coakley, Jr., J.E. Hansen, and D.J. Hofmann, 1992: Climate forcing by anthropogenic aerosols. *Science*, 255, 423-430.
- Clothiaux, E.E., et al., 1995: An evaluation of a 94-GHz radar for remote sensing of cloud properties. *J. Atmos. Oceanic Technol.*, 12, 201.
- Coakley, J.A., Jr., R.L. Bernstein, and P. A. Durkee, 1987: Effect of ship-stack effluents on cloud reflectivity. *Science*, 237, 1020-1022.
- Crane, R.G., and M.R. Anderson, 1984: Satellite discrimination of snow /cloud surfaces. *Int. J. Remote Sensing*, 5, 213-223.
- Curry, J. A., W. B. Rossow, D. Randall, and J. L. Schramm, 1996: Overview of Arctic cloud and radiation characteristics. *J. Climate*, 9, 1731-1764.
- Doutriaux-Boucher, M., and G. Seze, 1998: Significant changes between the ISCCP C and D cloud climatologies. *Geophys. Res. Lett.*, 25, 4193-4196.
- Dowling, D. R., and L. F. Radke, 1990 : A summary of the physical properties of cirrus clouds. *J. Appl. Meteor.*, 29, 970-978.
- Frouin R., and C. Gautier, 1988: Downward longwave irradiance at the ocean surface from satellite data: Methodology and in situ validation. *J. Geophys. Res.*, 93, 597-619.
- Gates, W. L., et al., 1999: An overview of the results of the Atmospheric Model Intercomparison Project (AMIP I). *Bull. Amer. Meteor. Soc.*, 80, 29-54.
- Hadley Centre, 1995 : *Modelling Climate Change, 1860-2050*, 1995.
- Han, Q., W. B. Rossow, and A.A. Lacis, 1994: Near-global survey of effective droplet radii in liquid water clouds using ISCCP data. *J. Climate*, 7, 465-497.
- Hansen, J. E., M. Sato, A. Lacis, R. Ruedy, I. Tegen, and E. Matthews, 1998: Climate forcings in the industrial era. *Proc. Natl. Acad. Sci. USA*, 95, 12753-12758.

- Harrison, F., P. Minnis, B. R. Barkstrom, V. Ramanathan, R. D. Cess, and G. G. Gibson, 1990: Seasonal variation of cloud radiative forcing derived from the Earth Radiation Budget Experiment. *J. Geophys. Res.*, **95**, 18687-18703.
- Houze, R. A. Jr., and P. V. Hobbs, 1982: Organization and structure of precipitating cloud systems. *Adv. Geophys.*, **24**, 225-315.
- Hughes, N. A., 1984: Global cloud climatologies: A historical review. *J. Climate Appl. Meteor.*, **23**, 724-751.
- Ignatov, A.M., L.L. Stowe, S.M. Sakerin, and G.K. Korotaev, 1994: Validation of the NOAA/NESIDIS satellite aerosol product over the North Atlantic in 1989. *J. Geophys. Res.*, **100**, 5123-5132.
- IGPO 1994: Utility and feasibility of a cloud profiling radar, IGPO Pub. Series 10, International GEWEX Program Office.
- IPCC 90, Climate Change 1990: The IPCC Scientific Assessment, 1990. Eds. J.T. Houghton, G.J. Jenkins and J.J. Ephraums, Cambridge University Press, 358pp.
- IPCC 95, Climate Change 1996: The Science of Climate Change, J. T. Houghton, L. G. M. Filho, B. A. Callander, N. Harris, A. Katterberg, and K. Maskell (eds.), Cambridge Univ. Press, 572pp.
- IPCC TAR, 1999: A preliminary version of the third report of IPCC.
- Jaenicke, R., 1993: Tropospheric Aerosols. In *Aerosol-Cloud-Climate Interactions*(Ed. Peter V. Hobbs), 1-31, Academic Press, San Diego.
- Kawamoto, K., T. Nakajima, and T. Y. Nakajima, 2000: A Global Determination of Cloud Microphysics with AVHRR Remote Sensing. submitted to *J. Climate*.
- King, M. D., Yoram J. Kaufman, W. Paul Menzel, and Didier Tanre, 1992: Remote Sensing of Cloud, Aerosol, and Water vapor Properties from the Moderate Resolution Imaging Spectrometer (MODIS). *IEEE Trans. Geoscience and Remote Sensing*, **30**, 2-27.
- Lemke, H., O. Danne, M. Quante and E. Raschke 1997 : "Study on critical requirements for a cloud profiling radar" final report ESTEC Conatct No. 11327/94/NL/CN
- Liou, K. N., 1992: *Radiation and Cloud Processes in the Atmosphere*, Oxford, New York, 487 pp.
- Liu, Z., P. Voelger, and N. Sugimoto, 2000: Simulation for the Observations of Clouds and Aerosols with the Experimental Lidar in Space Equipment (ELISE) submitted to *Appl. Opt.* (Liu, Z., P. Voelger, and N. Sugimoto, 1999: Simulation Study for the Experimental Lidar in Space Equipment (ELISE), Abstracts of Papers, International Laser Sensing Symposium, Fukui, Japan, pp. 271-272.)

- Lohmann, U., and J. Feichter, 1997: Impact of sulfate aerosol on albedo and lifetime of cloud: A sensitivity study with the echam gcm. *J. Geophys. Res.*, 102, 13685-13700.
- London, J., 1957: A study of the atmospheric heat balance. Final Report, Contract AF 19(122)-165 (AFCRC-TR-57-287, New York University, [ASTIN 117227]), 99p.
- Lubin, D., B. Chen, D. Bromwich, R. C. J. Somerville, W-H. Lee, and K. M. Hines, 1998: The impact of Antarctic cloud radiative properties on a GCM climate simulation. *J. Climate*, 11, 447-462.
- Mitchell, J. F. B., T. C. Johns, J. M. Gregory, and S. F. B. Tett, 1995: Climate response to increasing levels of greenhouse gases and sulphate aerosols, *Nature*, 376, 501-504 .
- Morcrette, J.J., and Y. Fouquart, 1986: The overlapping of cloud layers in shortwave radiation parameterizations. *J. Atmos. Sci.*, 43, 321-328.
- Nakajima, T., and M. D. King, 1990: Determination of the Optical Thickness and Effective Radius of Clouds from Reflected Solar Radiation Measurements. PART I: Theory. *J. Atmos. Sci.*, 47, 1878-1893.
- Okamoto, H., A. Macke, M. Quante and E. Raschke 1995 : Modeling of backscattering by non-spherical ice particles for the interpretation of cloud radar signals at 94GHz. An error analysis. *Contr. Atmos. Phys.*, 68, 319-334.
- Peixoto, J. P., and A. H. Oort, 1992: *Physics of Climate*, American Institute of Physics, New York, 520pp.
- Roads, J., S-C Chen, S. Marshall, and R. Oglesby, 1998: Atmospheric moisture cycling rate trends from model runs. *GEWEX News*, 8, August.
- Rossow, W.B., and R. A. Schiffer, 1991: ISCCP cloud data products. *Bull. Amer. Meteor. Soc.*, 72, 2-20.
- Rossow, W. B., L. C. Garder, P. J. Lu, and A. W. Walker, 1991: International Satellite Cloud Climatology Project (ISCCP): Documentation of cloud data, WMO/TD-No.266, World Meteorological Organization, 76pp.
- Rossow, W. B., A. W. Walker, and L. C. Garder, 1993: Comparison of ISCCP and other cloud amounts. *J. Climate*, 6, 2394-2418.
- Rossow, W. B., and R. A. Schiffer, 1999: Advances in understanding clouds from ISCCP. *Bull. Amer. Meteor. Soc.*, 80, 2261-2287.
- Rotstayn, L. D., 1999: Indirect forcing by anthropogenic aerosols: A global climate model calculation of the effective-radius and cloud-lifetime effect. *J. Geophys. Res.*, 102, 9369-9380 .

- Sasano, Y., and T. Kobayashi, 1995: Feasibility study on space lidars for measuring global atmospheric environment, No.4 (Final Report), F-82-'95/NIES, p.106.
- Schiffer, R. A., and W. B. Rossow, 1983: The International Satellite Cloud Climatology Project (ISCCP): The first project of the World Climate Research Program. Bull.Amer.Meteor. Soc., 64, 779-784.
- Scorer, R. S., 1989: Cloud reflectance variations in channel-3. Int. J. Remote Sensing, 10, 675-686.
- Slingo, A., and J. M. Slingo, 1988: The response of a general circulation model to cloud longwave radiative forcing I : Introduction and initial experiments. Q. J. R. Meteorol. Soc., 114, 1027-1062.
- Stamnes, K., R. G. Ellingson, J. A. Curry, J. E. Walsh, and B. D. Zak, 1999: Review of science issues, development strategy, and status for the ARM North Slope of Alaska-Adjacent Arctic Ocean Climate Research Site. J. Climate, 12, 46-63.
- Stowe, L. L., H. Y. M. Yeh, T. F. Eck, C. G. Wellemeyer, H. L. Kyle, and the Nimbus-7 Cloud Data Processing Team, 1989: Nimbus-7 global cloud climatology. Part II: First year results. J. Climate, 2, 671-709.
- Takemura, T., H. Okamoto, Y. Maruyama, A. Numaguchi, A. Higurashi, T. Nakajima, A study of simulating aerosol distributions of various origins with a numerical climate model  
J. Geophys. Res. (submitted 2000)
- Trenberth, K.E., 1997: Using atmospheric budgets as a constraint on surface fluxes. J. Climate, 10, 2796-2809.
- Voelger, P., Z. Liu, and N. Sugimoto, 1999: Effects of Multiple Scattering on the Retrieval of Optical Parameters from ELISE - Simulation Study, SPIE 3865, 172-177.
- Warren, S. G., C. J. Hahn and J. London, 1985: Simultaneous Occurrence of Different Cloud Types, J. Climate Appl. Meteor, 24, 658-667.
- Warren, S. G., C. J. Hahn, J. London, R. M. Chervin and R. J. Jenne, 1988: Global distribution of total cloud cover and cloud type amounts over the ocean. NCAR Tech. Note NCAR/TN-317+STR, DOE/ER-0406, 212p.
- Weatherald, R. T., and S. Manabe, 1980: Cloud cover and climate sensitivity. J. Atmos. Sci., 28, 305-314.
- Wigley, T.M.L., 1991: Cloud reducing fossil-fuel emissions cause global warming? Nature, 349, 503-504.

- Yamanouchi, T., and Kawaguchi, S., 1992: Cloud distribution in the Antarctic from AVHRR and radiation measurements at the ground. *Int. J. Remote Sensing*, 13, 111-127.
- Yamanouchi, T., and T. P. Charlock, 1995: Comparison of radiation budget at the TOA and surface in the Antarctic from ERBE and ground surface measurements. *J. Climate*, 8, 3109-3120.